LITHOGEOCHEMISTRY AND HYDROGEOCHEMISTRY OF URANIUM AND ASSOCIATED ELEMENTS IN THE TOMBSTONE BATHOLITH, YUKON, CANADA

M. A. Olade and W. D. Goodfellow
Resource Geophysics and Geochemistry Division
Geological Survey of Canada
Ottawa, Ontario

ABSTRACT

Tombstone batholith, a Cretaceous alkaline intrusion in the Selwyn Fold Belt of central Yukon has a syenite-monzonite core and a tinguaite border, and is host to uranium mineralization with fluorite, disseminated molybdenite, galena and scheelite. Vein-type Pb-Zn-Ag mineralization, probably genetically related to the intrusion, is localized within country rocks near the southern contact of the batholith.

As part of a uranium reconnaissance program, a geochemical study of the batholith was undertaken utilizing rocks, stream sediments and waters to investigate physical and chemical processes affecting primary and secondary dispersion in an alpine glaciated, high latitude environment in the northern Canadian Cordillera.

Petrochemical and petrographic data suggest that the uranium-bearing tinguaite in association with a volatile-alkali rich fluid phase was earliest to crystallize within a subvolcanic environment possibly accompanied by contemporaneous faulting. Uranium and associated metals (Mo, Pb, Th) are considered to have fractionated into a volatile-alkali rich fluid phase transported in the form of fluoride complexes or other mobile complex ions, with subsequent precipitation under reducing conditions and decreased volatile pressures.

Multi-element anomalies of U, Mo, Pb and F are strongly developed in stream sediments draining known mineralization and other potentially mineralized zones especially at the core of the batholith. Although the mode of secondary dispersion is dominantly mechanical, partial extraction studies and variation in Th/U ratios suggest a hydromorphic component especially for U and other soluble elements, mostly as precipitates on clays and organics. The lack of a strong development of U anomalies in stream waters draining the uraninite-bearing tinguaite, in contrast to streams draining the syenite core, is attributed to pH-HCO_3^- equilibria and the relative stability of uranium-hydroxyl complexes at the sediment-water interface. The strong anomalies found in stream sediments and waters at the core of the batholith are not known to be lithologically or environmentally controlled, and may represent a tinguaite source as yet unmapped and lying beneath glacial debris.

In the exploration for "porphyry-type" uranium mineralization in the Tombstone batholith, areas underlain by tinguaite are prime targets, especially where they are associated with multi-element stream sediment anomalies and other favourable geological indicators, including intense shearing and abundant fluorite and biotite.

INTRODUCTION

Recent interest in the so-called "porphyry" uranium deposits (Armstrong, 1974) has prompted a study of the close spatial, temporal and genetic association of such deposits with intrusive rocks. The Tombstone alkaline intrusive complex is host to uranium localized within a pseudoleucite tinguaite (a textural variety of phonolite), and disseminated tungsten and molybdenum within syenite and quartz

monzonite. The economic potential of the Tombstone area was noted in 1919 when Cockfield reported the occurrence of Ag-Pb-Zn veins in 'greenstone' and quartzite just south of the intrusion. Knight (1906) first described the pseudoleucite (an intergrowth of nepheline and K-feldspar) in samples collected by McConnell in 1904, and this was later discussed in detail by Tempelman-Kluit (1969). Stratigraphy and structure of rocks surrounding the batholith was mapped by Tempelman-Kluit (1970) and Green (1972). Garrett (1971) noted an anomalous U content in parts of the batholith. Gleeson and Jonasson in 1975 (Jonasson and Goodfellow, 1976) reported high U levels in streams draining the batholith.

The following summer, geochemical investigations were undertaken on detailed (Goodfellow and Jonasson, 1977) and reconnaissance (G.S.C. Open File 418) scales as part of the Uranium Reconnaissance Program (URP). The results of these studies outlined areas of U potential both within the Tombstone batholith and in other stocks of similar age and composition elsewhere in the Ogilvie Mountains, Yukon.

The present study, carried out in 1977 as a continuation of the work started in 1976, was intended to define the exact source and nature of the geochemical anomalies. It involved mapping of the compositional phases of the batholith, examination of the geological setting and probable style of mineralization and an evaluation of the use of stream sediments and waters in the exploration for porphyry uranium within the Tombstone batholith and rocks of similar composition elsewhere in the region.

This paper presents the results of integrated studies and a novel approach to the exploration for porphyry uranium, molybdenum and tungsten in the Tombstone batholith.

GENERAL GEOLOGY, PHYSIOGRAPHY AND SURFICIAL GEOLOGY

The Tombstone batholith, 45 kilometres north of Dawson City, lies in the Northern Plateau and Mountain area of the Canadian Cordillera (Bostock, 1961) (Figure 1) and comprises part of the Cloudy and Tombstone Ranges of the Ogilvie Mountains. The physiography is characterized by jagged ridges and spires commonly bounded by fault-controlled steep cliffs. Elevations reach 2150 m with a maximum relief of 1500 m. The physiography and surficial geology of the region have been described by Vernon and Hughes (1966) and the following is a summary of their findings.

The serrate ridges are separated by wide flat-bottomed U-shaped stream valleys filled with glacial and alluvial deposits to 1200 metre elevations. These deposits are locally derived and composed of sub-rounded to angular rock fragments. Although the area was not covered by continental glaciers during Pleistocene time its geomorphology is the product of alpine glaciation. Successive advances of valley glaciers originating along the north slope of the ridges deposited glacial material into the stream valleys. In certain areas, cirques were subjected to nivation and mass weathering which produced amphitheatre-shaped headwalls and sharp aretes. Small glaciers covered with rock debris still occupy cirques on the north slope of mountains. In other cirques, tarns mark the location of earlier alpine glaciers. The last advance of alpine ice occurred 7510 years ago (Vernon and Hughes, 1966).

The Tombstone area has a continental climate characterized by low precipitation and broad temperature ranges. Most streams, particularly in late spring and early summer, are fed by melting snow and ice and from groundwater. During spring run-off, silt-laden torrential streams flow down steep slopes and form extensive poorly sorted deltaic areas; the Tombstone River valley is the repository of thick alluvial and reworked glacial deposits. Silt-size sediment is found in small eddies, under boulders and near the stream bank. In areas where the stream is torrential and/or where the underlying rocks are resistant and contribute very little sediment to the stream system, moss which is commonly found along the stream bank serves to filter fine sediment from the stream water. The study area lies within the zone of discontinuous permafrost outlined by Brown (1960). Permafrost is generally restricted to north-facing slopes.

The regional setting of the Tombstone area is characterized by a thick miogeosynclinal succession of sedimentary and volcanic rocks ranging in age from Precambrian to Mesozoic (Tempelman-Kluit, 1970). The major lithologies consist of Precambrian to Cambrian quartz-pebble conglomerate, limestone, arkosic sandstone, maroon and green slate and mafic volcanic rocks overlain by chert and slate of Ordovician and Silurian age. Unconformably overlying the Precambrian and Lower Paleozoic rocks is a succession of Upper Paleozoic and Mesozoic rocks composed of Permian limestone, Triassic shale and limestone, Jurassic-Cretaceous slate and limestone. These rocks have been intruded by Lower Cretaceous diabase sills and dikes and mid-Cretaceous syenitic and monzonitic stocks and bathliths. The Tombstone

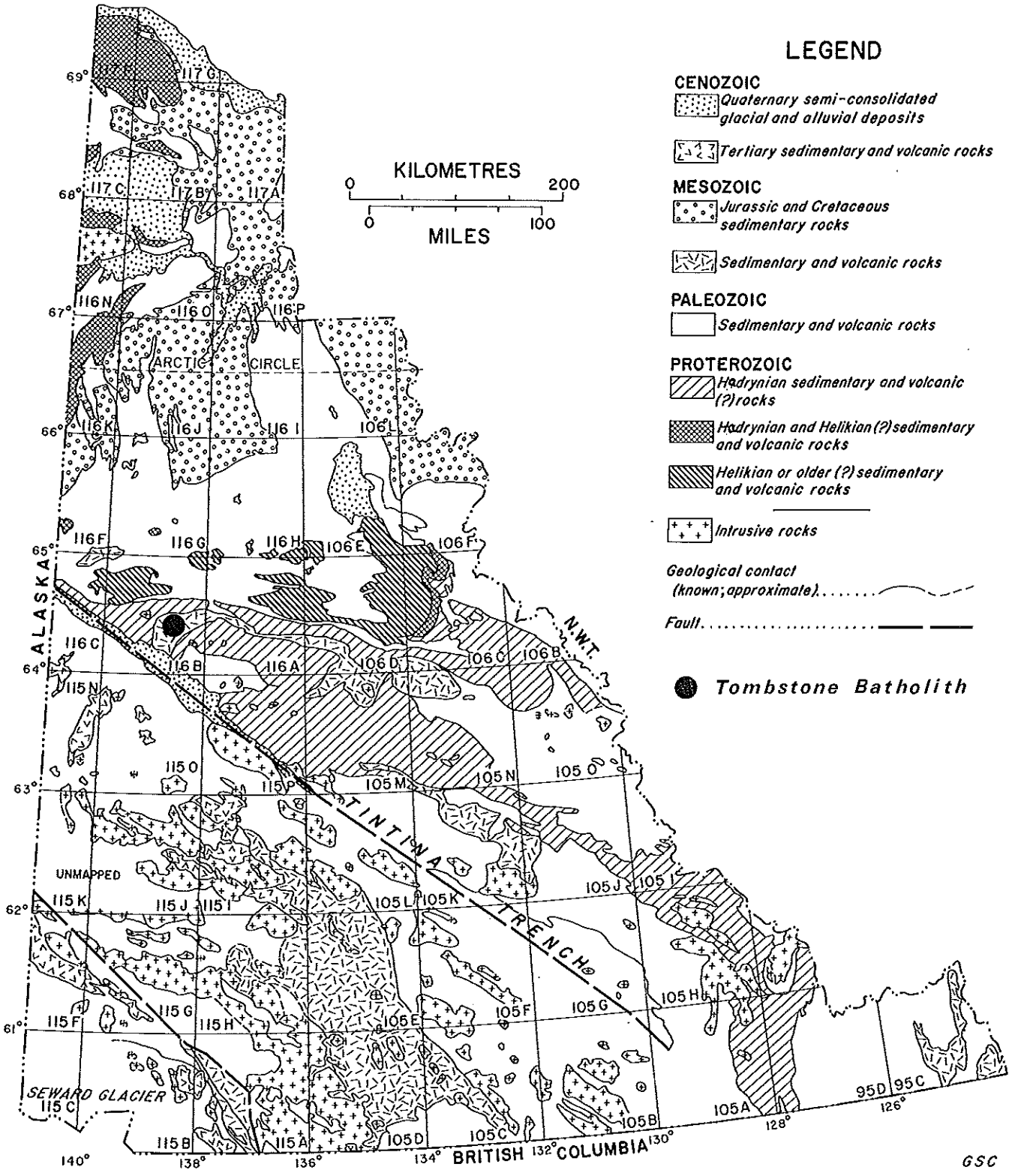

FIGURE 1. Geological map of Yukon Territory showing the location of the Tombstone batholith (after Findlay, 1972).

batholith, one of the latter, is discussed in greater detail below.

The structural geology of the area is characterized by folds and thrust faluts (Tempelman-Kluit, 1970). In the Tombstone area, structures trend north and northeast in the south and swing eastward in the north, defining a broad arc. Bedding parallels the structures and dips to the southeast. Most deformation predates the emplacement of late Cretaceous intrusions and most likely occurred in early Cretaceous time.

PETROLOGY

FIELD RELATIONSHIPS

The Tombstone batholith is a subcircular composite intrusion consisting dominantly of miaskitic alkali syenite (nordmarkite), with a southern border unit of pseudoleucite tinguaite and a core and marginal dike bodies of monzonite, quartz monzonite and granite (Figure 2). Where the syenite invades the Cretaceous diabase sheets, hybrid pyroxene diorite is developed. Near the centre of the batholith, a skarn zone occurs at the contact of the syenite with roof pendants or xenoliths of Permian limestone (now marble).

The pseudoleucite tinguaite is found, at the southern margin of the batholith where it forms a dike-like body up to 1 km wide between the syenite and Keno Hill Quartzite and near the core of the batholith where it appears as a small pipe-like body closely associated with other xenoliths of older country rocks (Figure 2). The monzonite and granitic rocks form the core of the batholith and also occur as a dike in the northern part of the intrusion (Figure 2), and as apophyses transecting the syenite at the core. A few felsite dikes (trachyte) occur within the syenite and locally cut the tinguaite.

Field relations indicate that the contact between the tinguaite and syenite in the southern part of the batholith is sharp and intrusive (Tempelman-Kluit, 1969) whereas that between the syenite and monzonite is gradational. There is no field evidence to support the view of Tempelman-Kluit (1969), that the tinguaite probably intrudes the syenite. To the contrary, in the southern part of the batholith, geologic mapping shows that the tinguaite body has been disrupted by the emplacement of the syenite. This is consistent with the observations of Knight (1906), and our observations of the gradational contact between the tinguaite and syenite at the second locality where the former is considered to be a "recrystallized" xenolithic body. Furthermore, the trachyte dikes which locally cut the tinguaite are possibly off-shoots from the syenite.

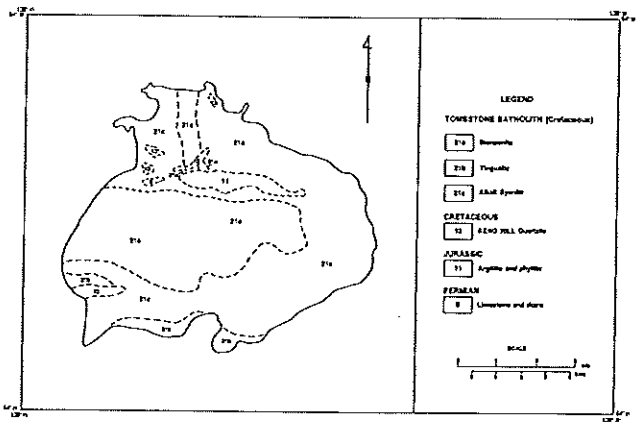

FIGURE 2. Geology of the Tombstone batholith showing the different compositional phases (modified after Tempelman-Kluit, 1970).

PETROGRAPHY

The petrography of rocks from the Tombstone batholith has been described by Knight (1906) and Tempelman-Kluit (1969, 1970). These descriptions are in many respects consistent with our observations on the examination of several thin and polished sections of fresh and mineralized samples, and the following is a summary of these findings.

TINGUAITE

The pseudoleucite tinguaite is porphyritic, and contains phenocrysts of pseudoleucite (intergrowth of nepheline and K-feldspar) and sanidine set in a fine-grained equigranular groundmass of nepheline, alkali feldspar, plagioclase and biotite, with fluorite, cancrinite, calcite, sphene, nosean, aegirine (?) and melanite (garnet) as accessories. Estimated modal proportions are alkali feldspar (60–65%), nepheline (15–20%), biotite (3–10%), plagioclase (2–3%) and accessories (3–5%). Alkali feldspar occurs both in the pseudoleucite 'patches' and groundmass as closely-packed equant to tabular orthoclase (approximately 0.1 mm) interlocked with nepheline, and less commonly as euhedral sanidine phenocrysts up to 3 cm long. Biotite, the dominant mafic mineral, varies in color from pale yellow to dark brown, and occurs as small interstitial flakes scattered or in clusters within the groundmass and miarolithic cavities. Accessory minerals include melanite (altered deep brown) with

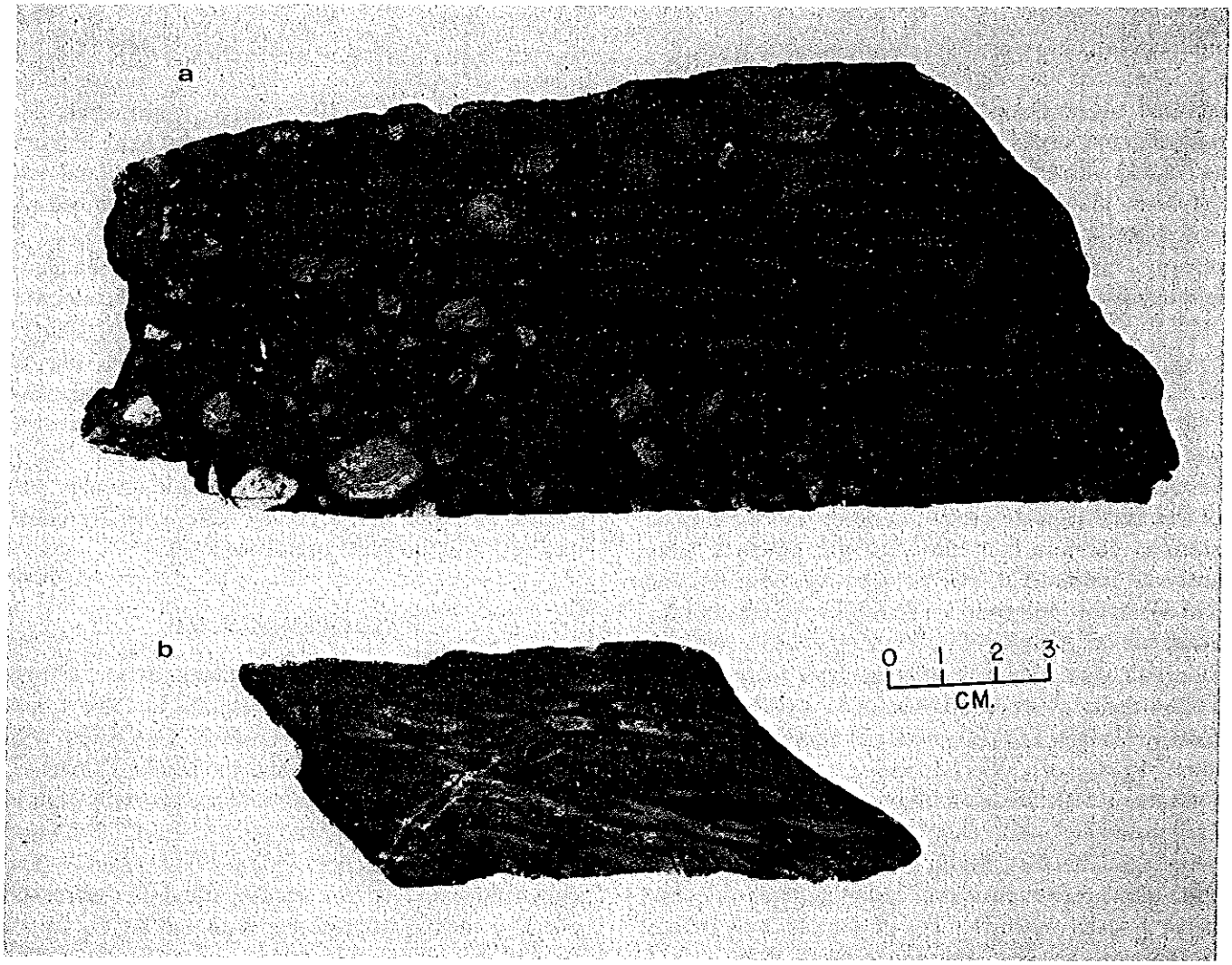

PLATE 1. Photograph of (a) unmineralized and (b) mineralized tinguaites.

borders of leucoxene, abundant fluorite crystals, interstitial calcite closely associated with fluorite secondary muscovite.

SYENITE

The alkali syenite is medium grained hypidiomorphic, ranging in texture from granular to porphyritic-trachytoid. Modal compositions which are extremely variable are estimated as follows; orthoclase (60–90%), plagioclase (0–20%), quartz (0–5%), pyroxene (1–15%), amphibole (0–10%), biotite (0–5%) and accessories (1–15%). Orthoclase-microperthite occurs as tabular grains about 3 cm long, and often with numerous inclusions of albite crystals and blebs (hypersolvus). Plagioclase of albite to oligoclase composition occurs dominantly as rims or inclusions in orthoclase as well as being interstitial. Pyroxene, the usual ferromagnesian mineral in the syenite is aegirine-augite and forms stout prismatic to anhedral grains closely intergrown with amphiboles (arfvedsonite and hornblende). Biotite is rare and mainly interstitial or a replacement of hornblende. Accessory minerals include melanite (locally up to 15%), eudialyte (Ti-rich zircon), abundant rhombic sphene, fluorite, calcite and sulphides.

MONZONITE, QUARTZ MONZONITE AND GRANITE

Monzonite is in part transitional to quartz monzonite and locally into granite. The rock is medium grained, hypidiomorphic granular to slightly porphyritic, consisting of subhedral to anhedral orthoclase (45–50%), plagioclase (25–30%), quartz (2–10%), pyroxene (0–10%), amphibole (5–15%), biotite (1–

10%) and accessory minerals (1–2%). Orthoclase is non-perthitic, and plagioclase is of andesine composition. Pyroxene (augite) is closely intergrown with and replaced by hornblende. Biotite forms lenticular to ragged grains usually brownish-green and commonly associated with hornblende.

Quartz monzonite and granite are similar to the monzonite in textural features, but only differ in possessing higher contents of quartz and lesser feromagnesian minerals.

SAMPLE PREPARATION AND ANALYSIS

Rock chip samples weighing approximately 2 kg were crushed in a Chipmunk jaw-crusher and pulverized to 20 mesh in a Braun ceramic disc mill. Splits of this material were ground to minus-150 mesh in an alumina ceramic ball mill. Sample powders were analyzed for Zn, Cu, Pb, Ni, Co, Ag, Mn, Fe, and Mo by atomic absorption spectrophotometry after decomposition with HF-$HClO_4$-HNO_3 acid mixture. Uranium was determined by delayed neutron activation using procedures developed by the Atomic Energy Canada Ltd., Commercial Products Division (Boulanger, *et al.*, 1975). Fluorine was determined by ion-selective electrodes following fusion with sodium carbonate-zinc oxide flux. SiO_2, Al_2O_3, FeO (expressed as total Fe), MgO, CaO, Na_2O, K_2O, TiO_2, P_2O_5 and MnO were determined by X.R.F. on a glass pellet formed by fusing 1 g of sample with lithium metaborate. Th was determined by X.R.F. on pelletized rock powders at Bondar-Clegg laboratories. CO_2 and S were determined by the standard Leco furnace combustion method.

Stream sediments were air-dried, disaggregated, sieved to minus-80 mesh and analyzed for Zn, Cu, Pb, Ni, Co, Ag, Mn, Fe, Ba, and Mo by atomic absorption spectrophotometry, following a hot leach with 4M HNO_3/M HCl. Tungsten was determined by colorimetry, U by delayed neutron activation, and F by specific ion electrode. Uranium was also determined in stream sediments by two partial extraction procedures. In the first procedure, 0.25 g sample was digested with 4M HNO_3/M HCl by the method of Smith and Lynch (1969), and 1 ml aliquots from the 10-ml solutions were analyzed by fluorometry. In the second procedure, 0.1 g sample was weighed into a 10-ml calibrated test tube. 1 ml of 30% H_2O_2 was added and allowed to stand for 1 hr after which 1 ml of deionized water was added and the test tube shaken for a minute. 8 ml of 2.5% Na_2CO_3 was subsequently added and the solution mixed in a sonic cleaner (Branson Instruments Co., Model D-100) for 1 hr. The solution was placed in a water bath at 90°C for 30 minutes to 'boil off' the excess H_2O_2. Sample solution was made up to 10-ml mark, centrifuged, decanted, and 1 ml aliquot was evaporated in a platinum dish, fused with a carbonate-fluoride flux and analyzed by fluorometry using procedures described by Smith and Lynch (1969).

Stream waters were collected unfiltered and analyzed in the field for U (fluorometry), F (selective ion electrode), pH and Cu (colorimetry). Subsequently, samples were analyzed for Ca, K, Na by atomic absorption, HCO_3^- by titration, and conductivity. Sulphate and Cl^- were also determined but were found to be generally below detection limits.

Using control standards and replicate samples, analytical precision and accuracy were generally better than ±15% at the 95% confidence level.

PETROCHEMISTRY

Major and minor-element contents of rocks from the Tombstone batholith are presented in Table 1, and as variation diagrams in Figure 3. Compared with average tinguaite, syenite and monzonite (Table 1), rocks of the Tombstone batholith are generally high in SiO_2, Al_2O_3 and K_2O, and poor in Na_2O, CaO and the femic elements (FeO, MgO, TiO_2, MnO). The enhanced SiO_2 is not accompanied by increased quartz contents, whereas the K_2O and Al_2O_3 values reflect the modal proportions of orthoclase. The Na_2O/K_2O ratio is generally less than one, an unusual feature in typical tinguaites (Johannsen, 1937) which reflects the subsolidus crystallization of nepheline from the breakdown of K-rich pseudoleucite, and the strong potassic affinity of the parent syenite magma.

A plot of the major elements on a Harker diagram using SiO_2 as a measure of differentiation (Figure 3a), shows that the tinguaite is the least differentiated, whereas the monzonite-granite is most fractionated. This is consistent with spatial relationships and mineralogical variations. K_2O, Na_2O and Al_2O_3 show a progressive decrease as SiO_2 increases, whereas for the femic elements, values increase from tinguaite to syenite and then decrease in the more silicic differentiates. The enhanced femic elements within the syenite reflect the greater abundance of mafic minerals.

Barium and strontium values are highest in the syenite, and on a Harker diagram (Figure 3b) show a distribution like the femic elements. Barium is not strongly correlated with K_2O (Table 1), but the high

TABLE 1.
COMPARISON OF MAJOR AND MINOR ELEMENT CHEMISTRY AND NORMATIVE COMPOSITIONS OF ROCKS FROM THE TOMBSTONE BATHOLITH WITH AVERAGE ROCKS OF SIMILAR COMPOSITION LOCATED ELSEWHERE.

	Tinguaite			Syenite			Monzonite			Granite		**Aver. Tinguaite	Aver. Syenite	Aver. Monzonite
	65010	66075	66074*	65007	65009	65003	65005	65006	65008	65004	65002	—	—	—
SiO_2	56.60	56.70	57.80	63.70	63.70	64.60	69.90	70.10	66.60	75.00	80.20	54.08	58.58	62.60
Al_2O_3	20.20	21.70	19.80	16.90	17.00	18.30	16.20	16.00	17.10	11.00	10.60	18.65	16.64	15.65
Fe_2O_3	1.00	1.30	0.20	2.40	1.10	1.10	0.90	0.10	1.10	2.10	0.00	3.92	3.04	1.92
FeO	1.80	1.30	2.80	2.30	2.20	0.10	1.10	1.00	1.60	1.70	1.30	2.28	3.13	3.08
MgO	0.26	0.21	0.45	0.53	0.66	0.09	0.34	0.31	0.08	0.00	0.08	1.07	1.87	2.02
CaO	0.97	1.30	1.20	1.44	2.22	1.04	1.64	1.70	0.92	0.20	0.51	2.77	3.53	4.17
Na_2O	4.70	6.60	0.90	3.60	5.10	7.70	3.10	3.80	3.80	2.90	1.60	8.10	5.24	3.73
K_2O	12.20	9.10	12.20	7.32	7.21	5.35	6.10	4.99	6.18	4.74	4.22	5.52	4.95	4.06
TiO_2	0.37	0.23	0.45	0.47	0.42	0.05	0.25	0.18	0.19	0.20	0.24	0.54	0.84	0.78
P_2O_5	0.06	0.07	0.14	0.15	0.11	0.04	0.08	0.06	0.02	0.04	0.05	0.20	0.29	0.25
MnO	0.09	0.17	0.08	0.07	0.10	0.01	0.05	0.02	0.07	0.05	0.02	0.22	0.13	0.10
CO_2	0.00	0.00	0.20	0.00	0.00	0.00	0.00	0.20	0.00	0.00	0.00	0.06	0.28	0.08
H_2O	0.50	0.40	1.10	0.60	0.20	0.20	0.30	0.60	0.40	0.30	0.30	2.33	0.52	1.09
S	0.70	0.46	0.18	0.08	0.14	0.14	0.03	0.09	0.14	0.05	0.04	—	—	—
Norms														
Q	—	—	1.76	10.72	1.67	—	24.74	25.56	18.49	39.98	53.38	—	0.86	14.18
c	—	—	3.85	0.79	—	—	1.81	1.89	2.59	0.84	2.62	—	—	—
cr	64.10	54.31	74.86	43.76	42.66	32.14	35.69	29.55	37.38	28.62	25.25	33.52	29.72	24.39
ab	—	14.78	7.90	30.78	43.17	61.58	26.33	32.62	32.87	25.04	13.69	26.12	45.00	32.06
an	—	2.71	3.91	6.22	2.18	—	7.64	6.87	4.53	0.74	2.22	—	7.36	14.18
lc	6.94	—	—	—	—	—	—	—	—	—	—	—	—	—
ne	19.65	22.51	—	—	—	2.02	—	—	—	—	—	22.09	—	—
ac	2.92	—	—	—	—	0.74	—	—	—	—	—	3.04	—	—
di	1.30	1.13	—	—	3.04	0.49	—	—	—	—	—	5.90	3.88	2.50
he	2.49	0.58	—	—	3.76	—	—	—	—	—	—	2.53	1.52	1.28
en	—	—	1.16	1.33	0.24	—	0.85	0.78	0.20	—	0.20	—	2.92	3.95
fs	—	—	4.16	1.44	0.34	—	0.89	1.32	1.59	1.06	1.97	—	1.31	2.33
fo	0.04	—	—	—	—	—	—	—	—	—	—	—	—	—
fa	0.09	—	—	—	—	—	—	—	—	—	—	—	—	—
wo	—	0.51	—	—	—	1.81	—	—	—	—	—	0.82	—	—
mt	—	1.90	0.31	3.51	1.59	—	1.31	0.15	1.63	3.11	—	4.31	4.47	2.82
il	0.71	0.44	0.89	0.90	0.79	—	0.48	0.35	0.37	0.39	0.46	1.05	1.62	1.51
ap	0.14	0.16	0.34	0.35	0.26	0.94	0.18	0.14	0.05	0.09	0.12	0.48	0.68	0.59
py	1.45	0.95	0.38	0.17	0.29	0.21	0.06	0.19	0.29	0.11	0.08	—	—	—
ns	0.13	—	—	—	—	—	—	—	—	—	—	—	—	—
cc	—	—	0.47	—	—	—	—	—	—	—	—	0.14	0.65	0.18

*Mineralized tinguaite
**Average values, 93 tinguaites, 102 syenites and 102 monzonites (after Le Maitre, 1976)

values in the syenites suggest that Ba preferentially substitutes for K in alkali feldspar instead of nepheline and micas; which accounts in part for the high K_2O in the tinguaite. Reverse behaviour explains the distribution of Rb which is highest in the tinguaite. Potassium/rubidium ratios are lower in the tinguaite and monzonite, suggesting a higher degree of fractination than in the syenite. Although Sr generally shows a coherent relationship with Ca, the high values obtained in the syenite suggest that Sr substitutes for K in alkali feldspar formed at relatively high temperatures. Zirconium concentrations are highest in the tinguaite and monzonite where they occur mostly as 'residual' and accessory zircon, respectively.

Geochemical variations within the batholith generally reflect compositional zoning in the following order; tinguaite → syenite → monzonite → granite (Figure 4). In the tinguaite, the dominant salic minerals are nepheline, sanidine and unalbitized orthoclase, whereas in the syenite, orthoclase is strongly albitized (microperthite) reflecting hypersolvus crystallization. In the monzonite a subsolvus two-feldspar phase is well developed in which cryptoperthitic orthoclase co-exists with andesine (plagioclase). The anorthite

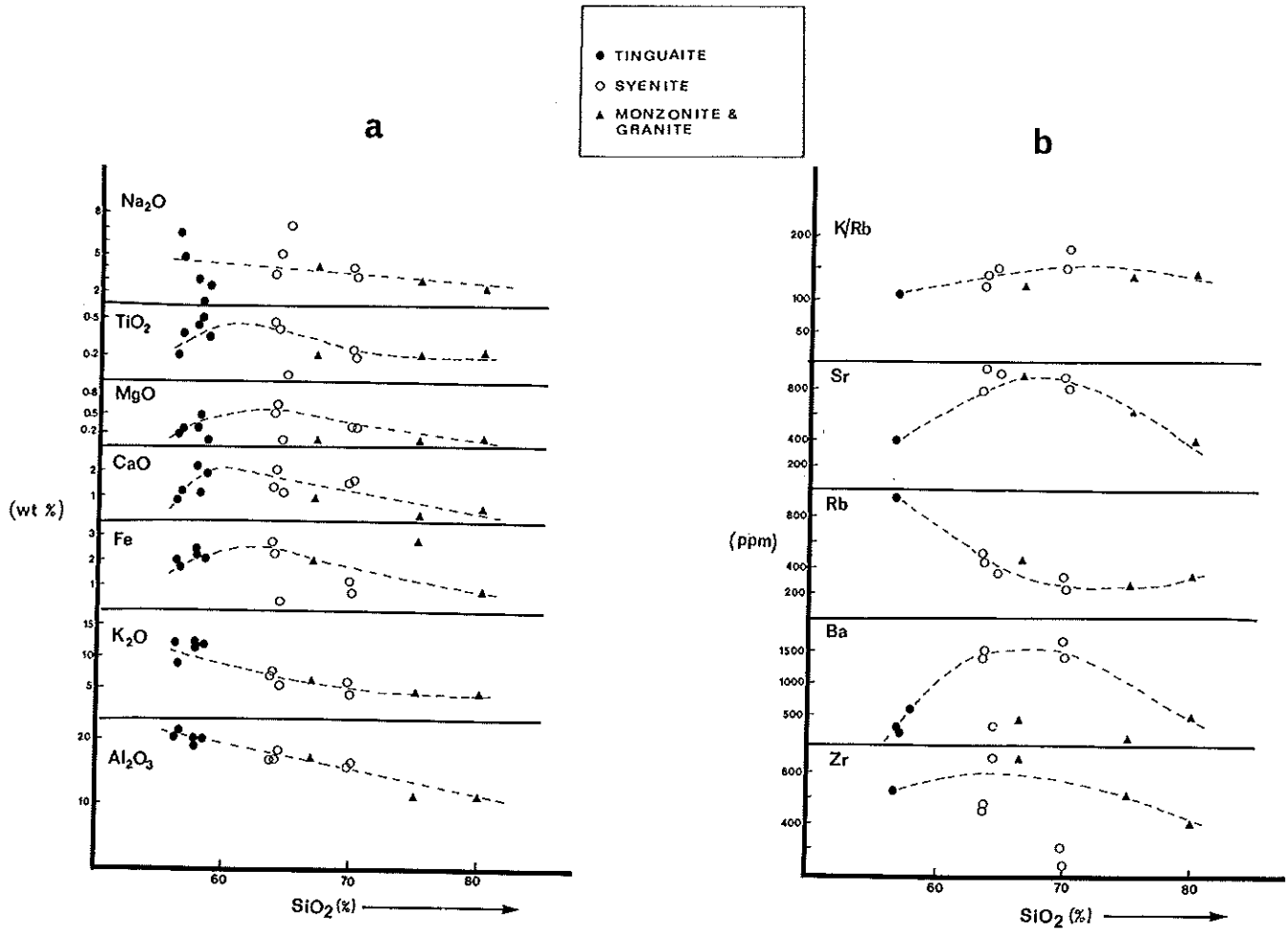

FIGURE 3. Harker diagram of major and minor elements plotted against SiO_2 for rocks from the Tombstone batholith.

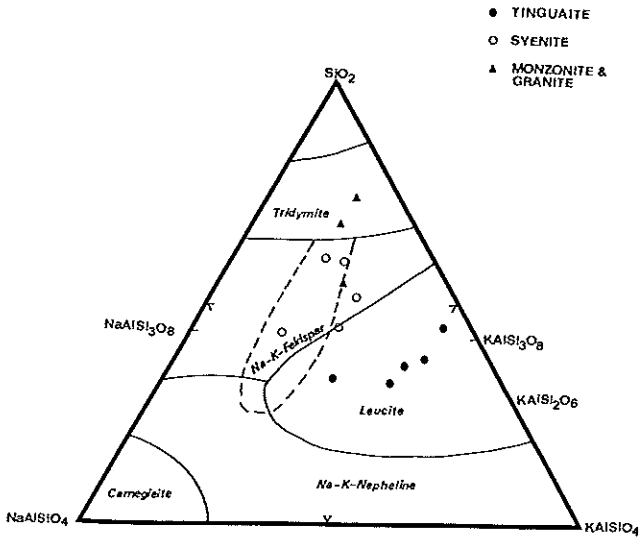

FIGURE 4. Normative compositions of tinguaite, syenite, monzonite, and granite plotted on a ternary $NaAlSiO_4$-$KAlSiO_4$-SiO_2 diagram.

content of the plagioclase also increases from syenite to monzonite. In the mafic minerals, biotite is dominant in the tinguaite, pyroxene and amphibole in the syenite, dominantly amphibole (with pyroxene and minor biotite) in the monzonite, and increasing biotite with decreased amphibole in the quartz monzonite and granite. Mineral composition also reflects the zonal relationships. Pyroxene is aegirine (rare) in the tinguaite, aegirine-augite in the syenite, and dominantly augite in the monzonite, reflecting decreasing Na content form margin to core. Amphibole in the syenite is mainly arfvedsonite whereas in the monzonite it is hornblende in composition. The compositional zoning with the Tombstone batholith is consistent with the proposition that the tinguaite is the earliest fraction or 'pulse' of the parent syenite magma to crystallize.

ORE MINERALOGY AND PETROGRAPHY

Uranium and related sulphide mineralization is localized dominantly within the tinguaite. In the tin-

guaite, uranium occurs as disseminations and veins of uraninite, and probably coffinite. These uranium-bearing minerals are closely associated with fluorite, molybdenite, galena and sphalerite. Under the microscope, uraninite occurs as crystals ranging from minute to 0.2 mm in size, either as inclusions within and between mineral grains, or in close association (inclusion and intergrowths) with dark-brown Fe-rich biotite which, when compared to unmineralized tinguaite, is relatively coarser (up to 0.5 mm), dark-brown (compared to pale-yellow) and rather more abundant (up to 15% of the mode). Cores of biotite are often dull-black, possibly due to metamictization. Secondary uranium mineralization, consisting of betafite and other uranium 'blooms,' is confined to silicified shear zones in the tinguaite near its contact with orthoquartzite. No extensive hydrothermal alteration zones have been noted, although compared with the fresh tinguaite, the mineralized rocks are slightly richer in SiO_2, K_2O, FeO, P_2O_5, MgO, CO_2, H_2O and F, and poorer in Na_2O, Al_2O_3 and Fe_2O_3. Uranium values generally range between 0.2 and 2% U_3O_8. The mode of occurrence of the uraninite as disseminations and its close association with biotite and accessory fluorite suggest a late magmatic/autometasomatic origin. The secondary mineralization is attributed to supergene remobilization and concentration.

U-Th-bearing accessory minerals within the syenite include sphene, eudialyte (zircon) and melanite (Ti-rich garnet). Molybdenite disseminations have been noted within the syenite, and scheelite in apophyses of the monzonite near the centre of the batholith. A felsite (trachyte) dike about 50 m long and 1 m wide, cuts the tinguaite near the southern contact of the batholith and contains minor fluorite, molybdenite and chalcopyrite. Oxidized zones containing pyrite and chalcopyrite occur along shear zones within the syenite near the northern part of the batholith. The Pb-Zn-Ag mineralization within country rock south of the batholith may be genetically related to the syenite intrusion.

EVOLUTION OF THE TOMBSTONE BATHOLITH

In the search for 'porphyry' uranium deposits, the evolution of the ore-bearing intrusive is important in understanding ore-forming processes. Geochemical and mineralogical variations suggest that the mineralized tinguaite was probably not a residual fraction of the magma. Differentiation trends within the Tombstone batholith are towards increasing SiO_2 and decreasing K_2O and Na_2O which are consistent with the late-stage monzonite-granite derivatives at the core of the batholith. Thus, the trends are from peralkaline to peraluminous, and undersaturated to oversaturated. The spatial and compositional zoning within the batholith are neither reverse nor fortuitous, but suggest that the tinguaite was the earliest phase to crystallize. This is supported by the fact that a trachyte dike of composition similar to the syenite cuts the sheared pseudoleucite tinguaite at the southern border of the batholith. Moreover, in the second locality near the centre of the batholith, tinguaite occurs as a xenolithic body enclosed within the syenite (Figure 2) close spatially to other xenolithic country rocks. Here, the tinguaite is coarser and its contact with the syenite is gradational, suggesting recrystallization and probably remelting by the still-fluid syenite magma.

The pseudoleucite tinguaite and alkali-volatile rich fraction or 'pulse' of the Tombstone syenite magma as evidenced by (1) high F, H_2O and CO_2 contents in the form of fluorite, interstitial biotite and calcite; (2) fluid-induced autometasomatic crystallization of cancrinite, sodalite, sericite (after nepheline), and dark brown and relatively coarse biotite; and (3) the presence of small miarolithic cavities filled with biotite clusters.

Textural and mineralogical features suggest that the tinguaite was emplaced at a shallow level within the crust. These features include porphyritic texture, miarolithic cavities, and sharp intrusive contacts with country rocks, which may indicate that the emplacement was contemporaneous with faulting and fracturing. Mineralogical banding within the syenite and porphyritic-trachytoid texture suggests epizonal crystallization of a magma with low viscosity. The unmixing of potash feldspar to micropertite in the syenite suggests that crystallization took place in a magma from which the volatiles have escaped, or in which they may have been used up in the formation of hydrous minerals. Thus, it seems the early crystallization of the biotite-bearing pseudoleucite tinguaite strongly depleted the volatile material in the magma. However, the transition from hypersolvus microperthite in the syenite to subsolvus two-feldspar crystallization in the monzonite suggests a gradual build up of water content in the residual magma (Tuttle and Bowen, 1958).

From the above discussion, it is apparent that the uraniferous tinguaite was an early 'pulse' of the syenite magma rich in alkalis and volatiles, emplaced at a high level subvolcanic environment induced probably by faulting, prior to the complete consolidation of the parent magma. The increased content of low molecular weight volatiles tended to lower the density of the

primary magma, and consequently promoted diffusion towards the cooler and lower pressure roof zones, surpassing the reverse effect of density gradients (Upton, 1960). Combined with the effects of contemporaneous faulting, this probably permitted the subvolcanic emplacement of the pseudoleucite tinguaite, and subsolidus breakdown of the leucite to orthoclase and nepheline. Experimental studies in the system $NaAlSiO_4$-$KAlSiO_4$-SiO_2-H_2O (Hamilton and Mackenzie, 1965) have shown that a trachytic (syenitic) magma can yield undersaturated (phonolitic or tinguaitic) and oversaturated (rhyolitic) liquids through an early crystallization of leucite or pseudoleucite (Figure 4). The nature of the associated ferromagnesian minerals also controls the course of crystallization of trachytic liquids. As noted by Currie (1976), the crystallization of leucite in the tinguaite slightly increases the agpaitic ratio in the syenite magma permitting the crystallization of sodic amphiboles and pyroxenes. The crystallization of these mafic minerals strongly reduces the agpaitic index of the residual melt permitting the crystallization of more calcic amphiboles, biotite and subsolvus feldspars within the later derivatives (monzonite, quartz monzonite and granite).

Uranium in alkaline magmas commonly fractionates into the alkali-volatile rich fluid phase (Shatkov, *et al.*, 1970; Bhose, *et al.*, 1974). Such a volatile-rich phase generally induces the oxidation of tetravalent uranium to the hexavalent form which is transported as UF_6 or mobile uranyl complex ions, and subsequently precipitated as uraninite and associated sulphides under slightly reducing conditions. This is consistent with the occurrence of uranium, fluorite and associated sulphides in the tinguaite. Thorium is generally not so mobile as uranium in alkali-rich fluids, and consequently may concentrate in accessory minerals in more saturated magma fractions. Molybdenum and tungsten have a strong affinity for oversaturated liquids, and are therefore expected to concentrate in more silicic differentiates of the syenite magma, such as in the monzonite and granite (Goldschmidt, 1954).

EXPLORATION GEOCHEMISTRY

ROCKS

Trace-element contents in rocks of the Tombstone batholith are summarized in Table 2. In the tinguaite, U concentrations are high and show a wide dispersion (3–264 ppm) which generally reflects its close genetic association with radioactive mineralization. Close to the mineralized zones, U values generally exceed 200 ppm, and commonly reach 10,000 ppm. These enhanced values are attributed to the occurrence of uraninite as disseminations and veins within the tinguaite. Uranium concentrations in the syenite range between 3 and 86 ppm, with an average of 18 ppm, which is similar to the average value of 14 ppm for rocks of similar bulk composition (Labhart and Rybach, 1971). However, a few values that exceed 40 ppm may suggest some association with discrete radioactive mineralization. Compared with the average value of 4 ppm U in granitic rocks, the monzonites and granites of the Tombstone batholith are enriched in U by a factor of 4, with a mean value of 16 ppm and a range of 2–60 ppm. This enhancement can be partly attributed to their more silicic nature and to the probable build-up of U during differentiation of the syenite magma.

Thorium concentrations generally show erratic distribution in the various rock units. Values in the tinguaite are more uniform, ranging between 55 and 124 ppm, with an average of 82 ppm. In the mineralized tinguaite, Th is high, reaching 1000 ppm; this may

TABLE 2
ARITHMETIC MEANS AND RANGES OF TRACE ELEMENTS IN TINGUAITES, SYENITES AND MONZONITES FROM THE TOMBSTONE BATHOLITH

	Tinguaite (Fresh) (12)*	Tinguaite (Mineralized) (1)	Syenite (25)	Monzonite (16)
Zn	110 (78–366)	117	96 (42–231)	53 (12–149)
Cu	8 (4–34)	17	10 (3–47)	5 (4–10)
Pb	108 (49–290)	206	48 (28–102)	36 (8–80)
Ni	3 (1–18)	2	3 (1–10)	3 (1–9)
Co	5 (1–18)	4	6 (3–18)	3 (1–6)
Ag	0.2 (0.1–0.4)	0.4	0.3 (0.2–0.5)	0.2 (0.1–0.2)
Mn	746 (614–1272)	705	762 (279–2125)	382 (42–819)
Mo	20 (2–138)	500	6 (2–12)	5 (1–550)
U	76 (3–264)	10,151	18 (3–86)	16 (2–60)
F	2200 (700–8000)	1,100	1162 (3–3200)	1351 (151–5150)
Th	82 (55–124)	995	102 (1–902)	102 (1–497)
W	2 (1–6)	—	2 (1–4)	3 (1–40)

*Number of samples in parentheses

reflect the substitution of Th for U in uraninite. Values in the syenite are extremely erratic (1–902 ppm), reflecting the varying abundance of accessory minerals, such as eudialyte, sphene, and melanite. A similar distribution applies to the monzonites where values range between 1 and 497 ppm. Thorium and uranium show a positive correlation in the overall phases of the batholith, which reflects their geochemical affinities during magmatic and post-magmatic processes. Thorium/uranium ratios generally cluster around 5:1, which is the normal range for syenitic rocks (Labhart and Rybach, 1971), (Figure 10). However, close to mineralization, the Th/U ratios decrease significantly to values between 1:2 and 1:10.

Fluorine shows a pattern similar to U, with the highest values in the tinguaite. A plot of U vs F (Figure 5) shows a positive correlation consistent with the strong preference of U for volatile melts rich in fluorine, and in accordance with the abundance of fluorite in the rocks. Mo values are similar in the Tombstone rocks, with a general range of 2–12 ppm, although a few high values in the tinguaite and monzonite exceeding 40 ppm and up to 550 ppm (Table 2) reflect the occurrence of disseminated molybdenite in the rocks. W at background levels ranges between 1 and 6 ppm, but anomalous values exceeding 30 ppm are associated with monzonite and granitic rocks probably containing disseminated scheelite in association with molybdenite disseminations. Pb values are high in rocks of the Tombstone batholith compared with the average values of 14 ppm for phonolites and nepheline syenites (Sahl, *et al.*, 1974). The tinguaite containing 49–290 ppm is associated with galena vein mineralization in the southern part of the batholith. Pb within the syenite (28–102 ppm) is within the range for rocks of corresponding alkali feldspar content, although one sample with 102 ppm Pb may be associated with mineralization. Moreover, the occurrence of Pb-Zn-Ag veins in country rocks (Figure 6) south of the batholith, may represent epithermal emanations from the Tombstone batholith. Zn values are relatively high, and their positive correlation with Pb values suggests an association of sphalerite with galena. Cu, Co, and Ni contents are erratic but generally within the range for normal igneous rocks of similar composition.

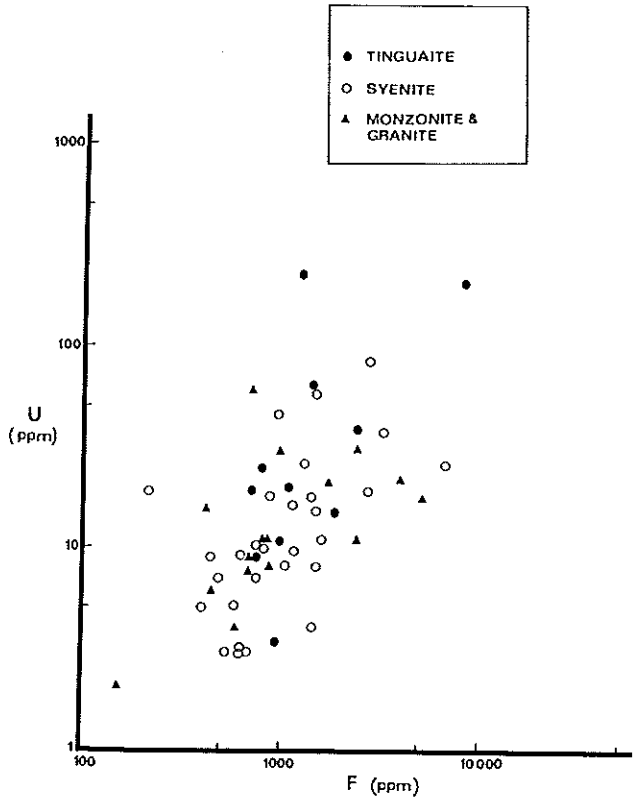

FIGURE 5a. Binary plot of U and F for rocks from the Tombstone batholith.

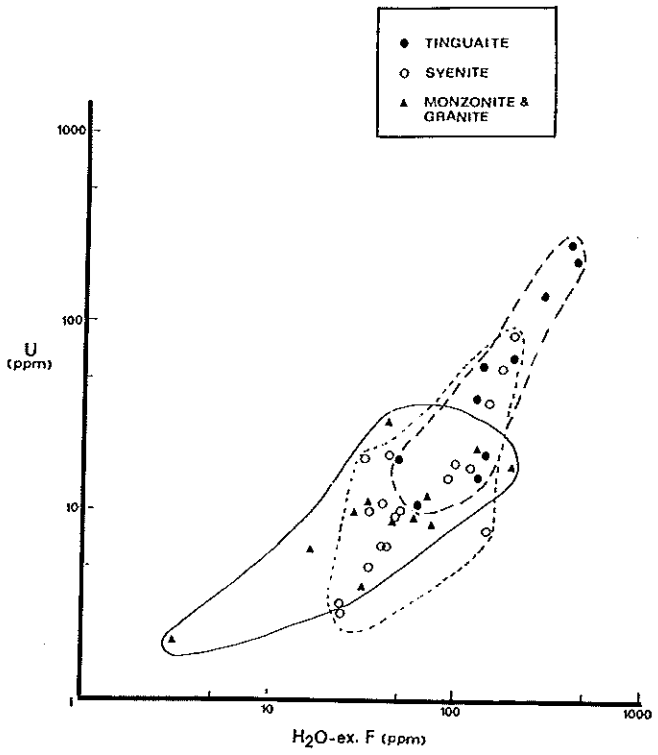

FIGURE 5b. Binary plot of H_2O-extractable F and total U for rocks from the Tombstone batholith.

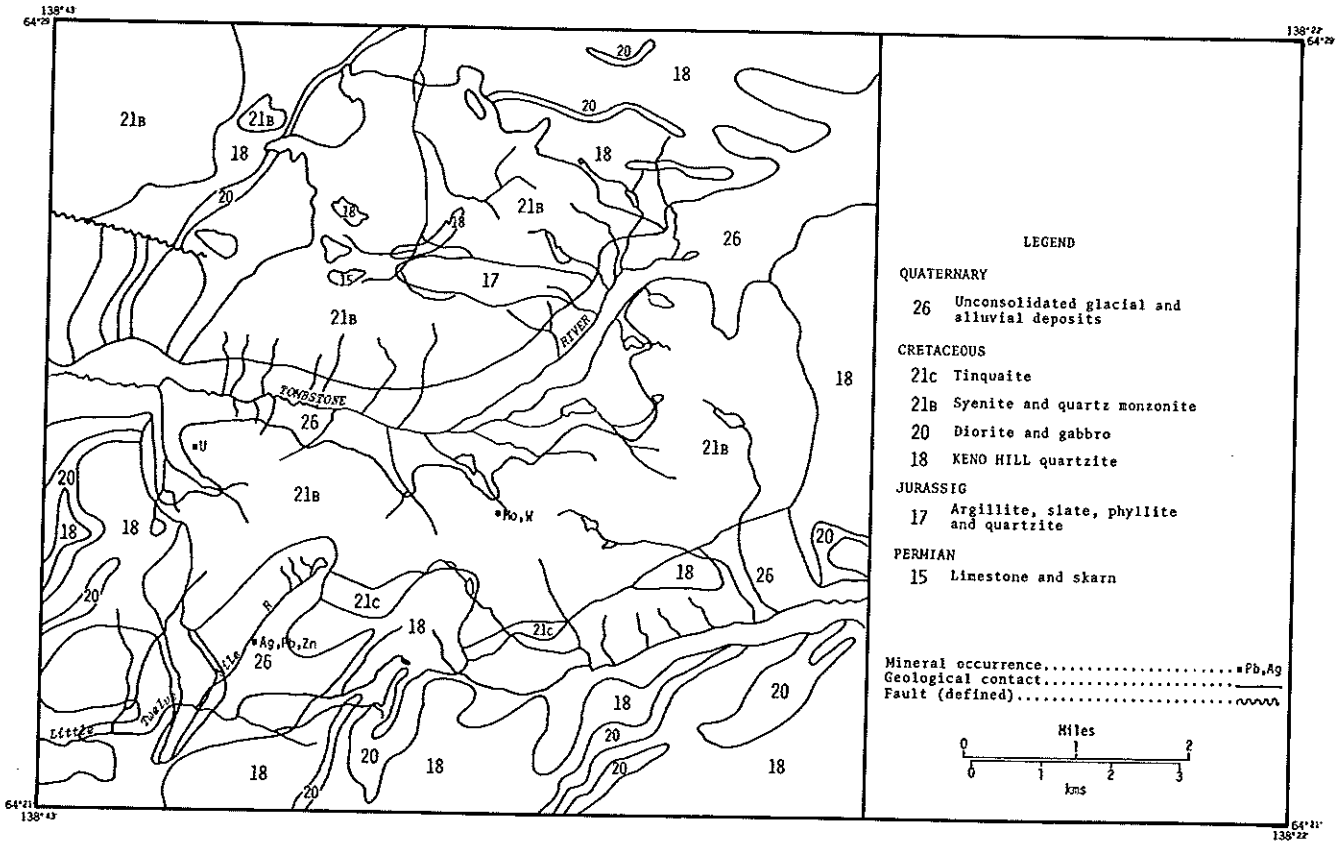

FIGURE 6. Geology of the Tombstone batholith and surrounding area showing the drainage and location of mineral occurrences (after Tempelman-Kluit, 1970; Green, 1972).

STREAM SEDIMENTS

Stream sediments derived from the Tombstone batholith by the abrasive action of streams, and in certain areas by alpine glaciation, are composed of variable proportions of accessory and major minerals reflecting the underlying lithologies. The minus-80 mesh fraction of stream sediments contains quartz (40–45%), feldspar (25–48%), pyroxene and amphibole (1–7%), biotite (2–18%), garnet (0–2%), sphene (0.5–6%), zircon (0–0.4%), and sulphides (0–0.2%). In streams draining U mineralization, uraninite is intimately associated with dark brown biotite. The mineral fragments in some samples are cemented with ferric hydroxide. Although most sediment samples contain some organic material, presumably derived from moss that served to trap fine sediment, the organic matter content is generally less than ten percent. Examination of the silt-sized fraction indicates that most of the organic material is composed of chemically inactive portions of living plants and is therefore unlikely to play an important role in the deposition and concentration of elements in stream sediments.

The distribution of U (Figure 7) in the minus-80 mesh fraction of stream sediment outlines three areas of high U content. There is a positive U anomaly associated with the tinguaite that forms a border phase located at the southern contact of the batholith. This is not surprising considering the presence of several U occurrences (mostly uraninite) associated with tinguaite in this area. A second area of high U concentration is located near the northern section of the batholith where tinguaite occurs wedged between xenoliths of Jurassic shale. A third U anomaly is located near the core of the batholith and is underlain by syenite and monzonite. This anomaly is more intensive and extensive than the first two, although a mineralized source for U has not been found to date. The U anomaly reaches concentrations greater than 500 ppm with a dispersion train measuring up to three kilometres. From leachability studies on the minus-80 mesh fraction of stream sediment after both H_2O_2-Na_2CO_3 and HNO_3 decompositions, it is clear that most of the U in anomalous stream sediments is in a very soluble form (Figures 8 and 9). The uranium occurs as uraninite and as molecules adsorbed onto the surfaces of mineral grains comprising the bulk of the

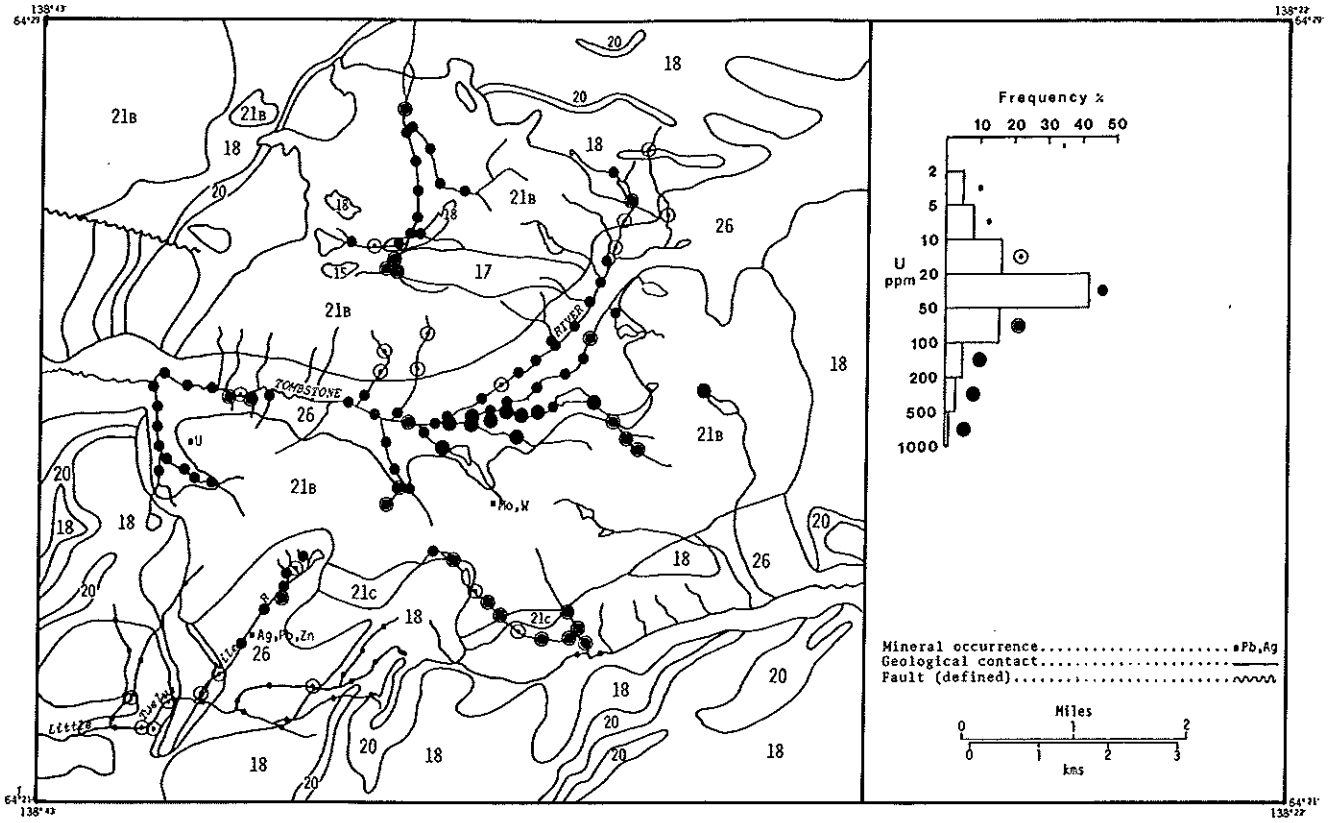

FIGURE 7. Distribution of U in sediments (minus-80 mesh) from streams draining the Tombstone batholith.

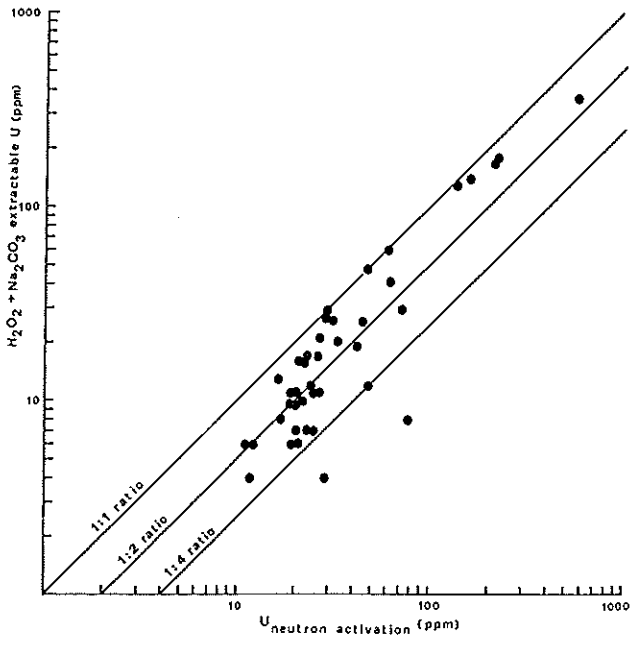

FIGURE 8. Binary plot of (H_2O_2+Na_2CO_3)-extractable U and total U in sediments from streams draining the Tombstone batholith.

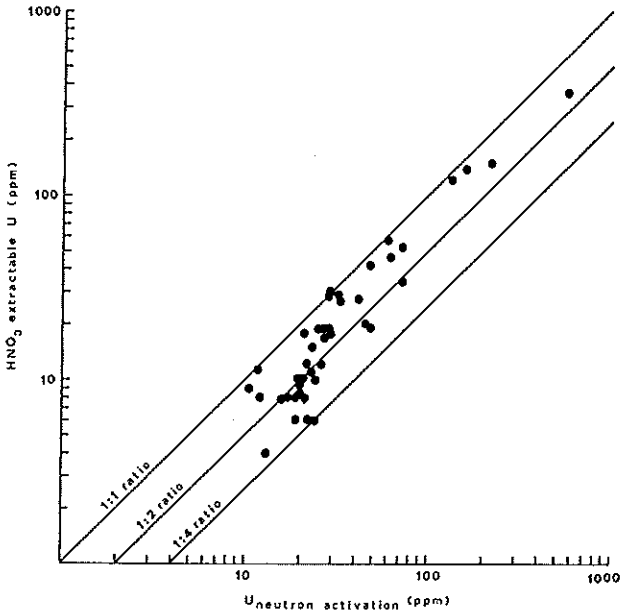

FIGURE 9. Binary plot of HNO_3-extractable U and total U in sediments from streams draining the Tombstone batholith.

sediment. This contrasts with U in sediments from background areas where most of the U is present in relatively resistant silicates and oxides, sphene and zircon. The U content of sediments from background areas is comparable to the U content of the underlying rocks (Table 3).

Elements associated with U mineralization in the Tombstone batholith include Th, Mo, Pb, F and, in one area, W. In general, there is a positive correlation of Th with U in syenite, monzonite, and tinguaite comprising the Tombstone batholith (Figure 10). The Th:U ratios range from a high of 10:1 in rocks unmineralized with respect to U to a low of 1:10 in mineralized tinguaites. This decreasing Th:U ratio in the mineralized tinguaites reflects the relative inability of Th to migrate any great distance, even as a fluoride complex and under elevated temperatures. The stream sediments on the other hand have Th:U ratios rarely in excess of 1:1 and decrease to 1:10 in areas of anomalously high U. This increase in U:Th ratios in the stream sediments demonstrates that U has been fractionated from Th by surficial processes. The separation and concentration of U relative to Th may be attributable to the high solubility of U relative to Th in stream waters, which may result from the mechanical dispersion and concentration of high-U, low-Th minerals such as uraninite, or may result from a combination of both. Evidence supporting a uraninite source for at least a portion of the high U present in sediments from anomalous areas includes the presence of significant quantities of uraninite associated intimately with dark brown biotite in the heavy portion of these sediments.

Other elements associated with U in the mineralized tinguaites and stream sediments are Mo, Pb, and F. The spatial distribution of Mo (Figure 11) corresponds to areas of high U. The high Mo in streams draining the tinguaite reflects the anomalous contents of Mo (up to 400 ppm) in the mineralized rocks (Table 2). In sediments from streams intersecting the core of the batholith, the Mo content ranges up to 100 ppm due to the presence of molybdenite in felsic dikes cutting the syenite.

In certain areas, such as near the core of the batholith and along the southern contact area, W appears spatially associated with areas of high U (Figure 12). Near the core of the batholith, the high W reflects the presence of scheelite associated with felsic dikes. The lack of a direct W-U association in the U-bearing tinguaites (Table 4) suggests that the W is not spatially

TABLE 3.
STATISTICAL DATA FOR STREAM SEDIMENTS AND WATERS, TOMBSTONE BATHOLITH, YUKON TERRITORY.

	Geometric Mean	Arithmetic Mean	Log Standard Deviation	Range	Unit	No. of Samples
Sediments:						
Zn	105.	119.	.21	36 – 345	ppm	166
Cu	36.7	47.2	.29	8 – 390	ppm	166
Pb	43.8	73.7	.28	13 –1040	ppm	166
Ni	15.4	18.7	.28	1 – 83	ppm	166
Co	9.6	12.5	.27	2 – 136	ppm	166
Ag	0.16	0.27	.36	0.1 – 3.6	ppb	166
Mn	428.	483.	.20	115 –3000	ppm	166
Fe	2.20	2.32	.14	1.00– 5.85	pct	166
Ba	1180.	1220.	.10	700 –2250	ppm	164
Mo	3.6	6.1	.41	1 – 87	ppm	166
W	6.3	12.8	.49	2 – 200	ppm	165
Hg	40.2	44.4	.19	10 – 150	ppb	100
U	28.6	47.1	.41	3 – 578	ppm	168
Waters:						
U	0.12	0.28	.61	.02– 2.2	ppb	173
F	172.	244.	.43	10 – 690	ppb	172
Cu	0.70	1.02	.31	0.50– 8.0	ppb	98
pH	—	7.1	—	6.2 – 7.9	—	173
Ca	3.86	5.7	.37	0.3 – 39.6	ppm	92
K	0.11	0.2	.55	0.05– 3.3	ppm	92
Na	1.14	1.8	.37	0.3 – 22.0	ppm	92
HCO_3	8.49	12.6	.38	1.4 – 77.5	ppm	92
Conductivity	—	38.4	—	7 – 259	μMhos	92

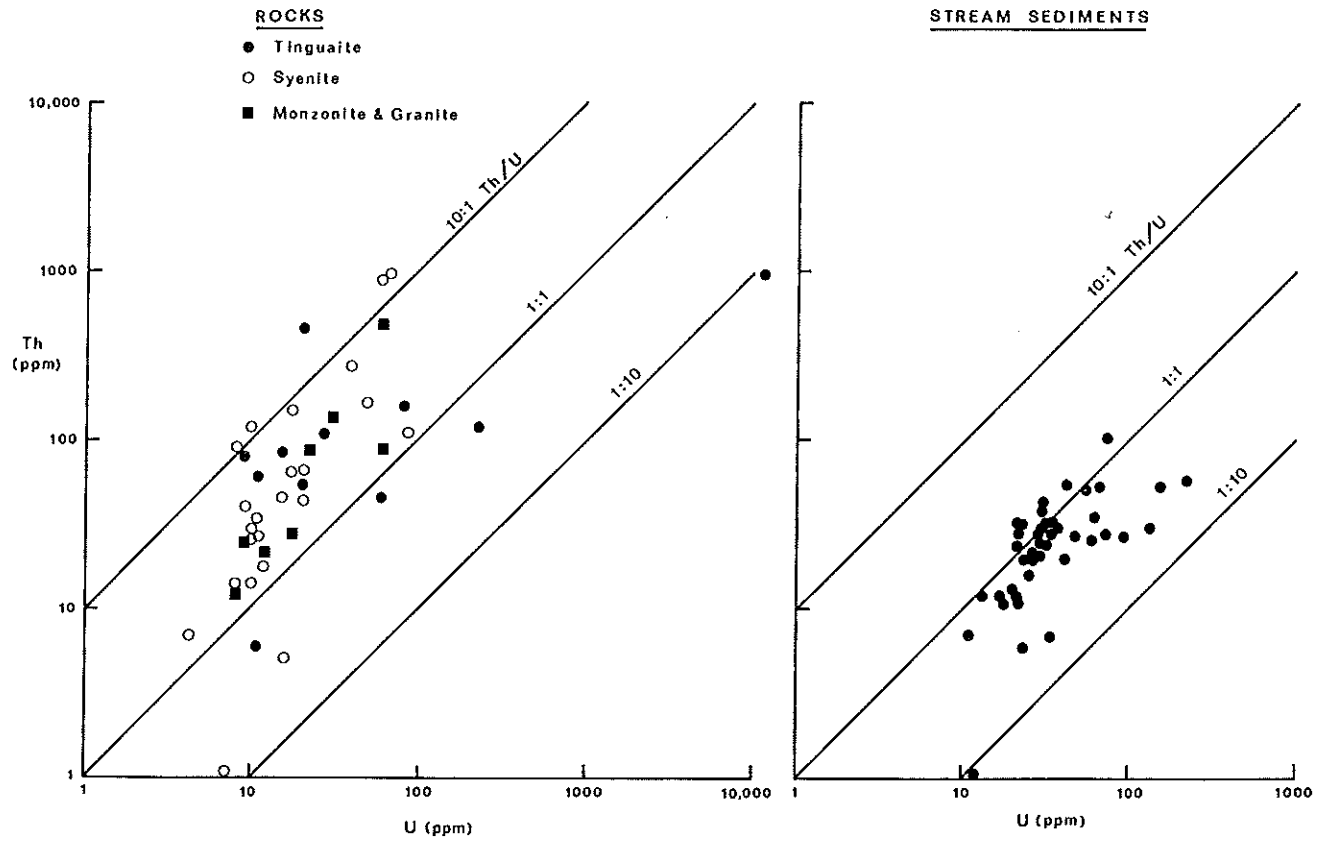

FIGURE 10. Binary plots of Th (X.R.F.) and U (delayed neutron activation) for rocks and stream sediments from the Tombstone batholith.

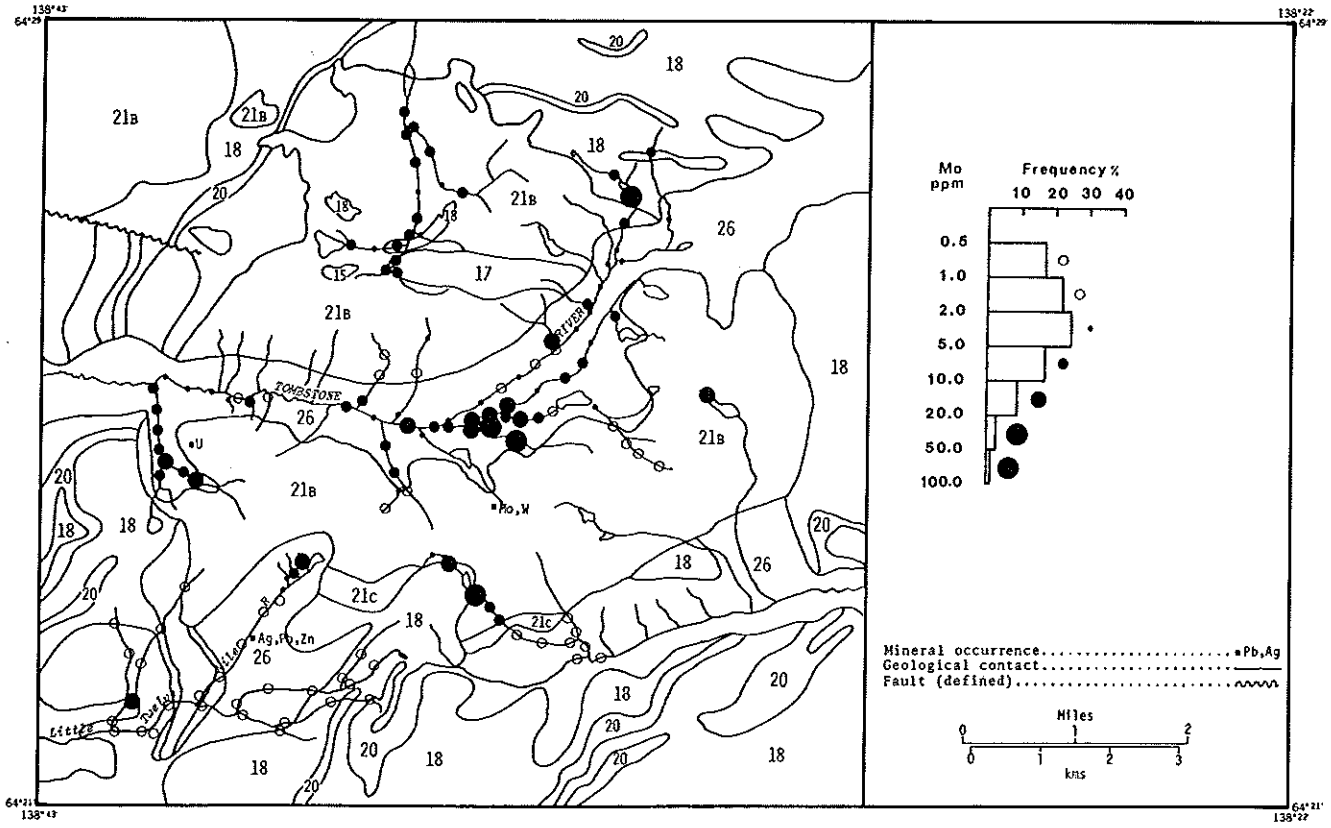

FIGURE 11. Distribution of Mo in sediments (minus-80 mesh) from streams draining the Tombstone batholith.

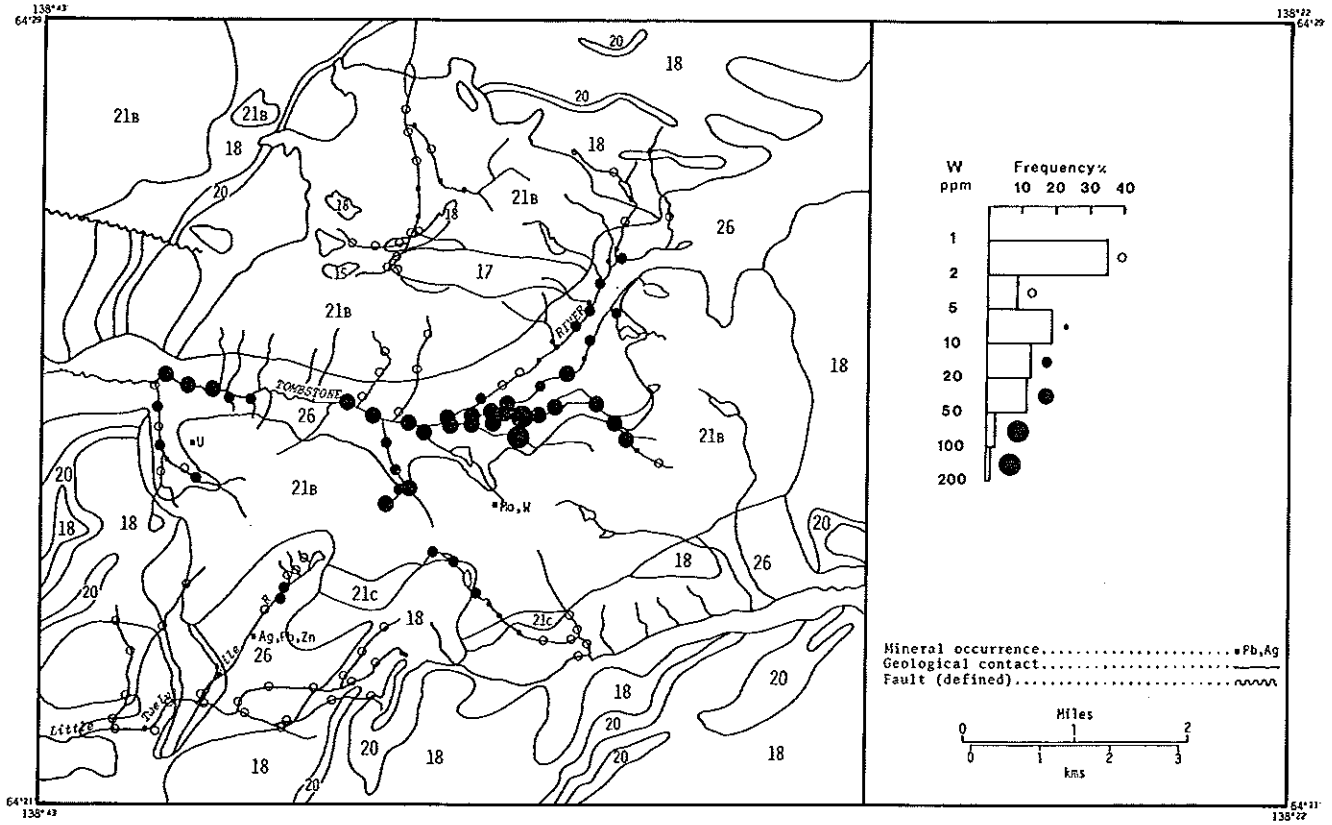

FIGURE 12. Distribution of W in sediments (minus-80 mesh) from streams draining the Tombstone batholith.

associated with mineralized rocks. Instead, the high W appears to be associated with the less alkaline syenite-monzonite phase of the intrusion. The relation is consistent with the interpretation that the tinguaite represents the earliest and therefore least differentiated halogen-rich phase of the batholith. Elements such as W that form refractory oxides would be expected to be retained in the parent magma.

Galena occurs in veinlets intersecting the pseudoleucite tinguaite. This association is apparent from the high Pb in the U-bearing tinguaite (Table 2) and from the distribution of Pb in the stream sediments (Figure 13). Almost without exception, areas of high U in the streams are underlain by the tinguaite occurring as a border phase along the southern contact and wedged between Jurassic shale in the northern sector of the batholith. Near the core of the batholith there is only a weak association of Pb with high U. The abnormally high Pb (greater than 1000 ppm) associated with Ag and Zn in sediments from streams draining the southwestern contact reflects the presence of Ag-Pb-Zn (Spotted Fawn Property) mineralization (Figure 13) known to occur in veins intersecting orthoquartzite and diabase (Cockfield, 1919).

The distribution of most of the remaining elements determined in the stream sediments (e.g. Cu, Zn, Co, Ni, Mn, Fe, and Ba) is controlled by the chemistry of the underlying rocks. The low Mn and Fe, except in areas underlain by early Cretaceous diorite and gabbro outside the batholith, are comparable to Mn and Fe levels in the underlying syenite, monzonite, and granite. Sediments from streams draining the tinguaite, however, are generally higher in Fe, reflecting the higher contents of ferrous Fe present as pyrite in the tinguaite (Table 1). The close similarity of Mn and Fe contents in the sediments and the underlying rocks demonstrates that these elements have been dispersed mechanically and that Mn and Fe hydroxides have not played a major role in scavenging and concentrating trace metals from stream waters. The high correlation of Co, Ni, Cu, and Zn with Mn and Fe (Table 4) is due to the close association of these elements with older gabbros and diorites that are intruded by the Tombstone batholith.

STREAM WATERS

The distribution of U in stream waters (Figure 14) outlines intensive (greater than 1 ppb) and extensive anomalies in streams draining the syenite core of the

TABLE 4.
CORRELATION MATRIX OF CHEMICAL DATA FOR STREAM SEDIMENTS AND WATERS FROM THE TOMBSTONE BATHOLITH.

(number of samples in parentheses)

	pH	F-W	U-W	U	Hg	W	Mo	Ba	Fe	Mn	Ag	Ni	Co	Pb	Cu
Zn	.25 (163)	-.04 (157)	-.25 (118)	-.01 (166)	.13 (100)	-.36 (102)	-.11 (136)	-.30 (164)	79 (166)	.70 (166)	.43 (51)	.63 (166)	.54 (166)	.73 (166)	.63 (166)
Cu	.01 (163)	-.31 (157)	-.14 (118)	-.07 (166)	.08 (100)	-.46 (102)	.19 (136)	-.15 (164)	.80 (166)	.47 (166)	.13 (51)	.81 (166)	.71 (166)	.28 (166)	
Pb	.20 (163)	.07 (157)	-.07 (118)	.11 (166)	.24 (100)	-.26 (102)	.01 (136)	-.22 (164)	.43 (166)	.51 (166)	.80 (51)	.17 (166)	.03 (166)		
Co	.14 (163)	-.42 (157)	-.33 (118)	-.31 (166)	.06 (100)	-.34 (102)	.18 (136)	-.37 (164)	.72 (166)	.35 (166)	-.02 (51)	.84 (166)			
Ni	-.01 (163)	-.33 (157)	-.26 (118)	-.17 (166)	.11 (100)	-.40 (102)	.18 (136)	-.21 (164)	.80 (166)	.59 (166)	.01 (51)				
Ag	.30 (50)	.02 (49)	-.30 (30)	-.23 (51)	-.24 (39)	-.25 (30)	-.23 (42)	-.03 (51)	.26 (51)	.24 (51)					
Mn	.01 (163)	.08 (157)	-.06 (118)	.15 (166)	.26 (100)	-.15 (102)	.23 (136)	-.23 (164)	.65 (166)						
Fe	.02 (163)	-.26 (157)	-.23 (118)	-.10 (166)	.07 (100)	-.33 (102)	.27 (136)	-.34 (164)							
Ba	-.12 (161)	.24 (155)	.46 (117)	.17 (164)	-.13 (100)	.06 (102)	-.15 (136)								
Mo	.29 (133)	.25 (129)	.27 (98)	.65 (136)	.40 (80)	.43 (94)									
W	-.30 (100)	.42 (99)	.31 (81)	.61 (102)	.30 (60)										
Hg	-.18 (97)	.04 (91)	.31 (77)	.32 (100)											
U	-.33 (165)	.63 (159)	.51 (120)												
U-W	-.37 (127)	.26 (124)													
F-W	-.15 (167)														

batholith. This U anomaly is coincident with an intensive U anomaly in the stream sediments. The U content of waters from streams intersecting the uraninite-bearing tinguaite located at the southern contact of the batholith, however, approaches background concentrations and is in general comparable to the lower U content of streams in this area.

For the pH range of waters from streams draining the Tombstone batholith, the UO_2^{+2} would be expected to be in hydrolysate form. Although the pH is controlled by carbonate equilibria, the CO_3^{-2} concentration is too low to complex significant quantities of U by forming $UO_2(CO_3)_2^{-2}$ (Langmuir and Applin, 1977).

In streams draining the syenitic core where there is a strong U response in the waters and sediments (Figures 7 and 14) and the pH is generally equal to or less than 7.0, $UO_2(OH)^+$ is the most likely U complex. The coincident U anomaly in both sediments and waters may result from the adsorption of U from solution onto the surfaces of minerals. Minerals such as micas and clays which have a large surface charge density will be most effective in adsorbing significant quantities of U from solution. In the case of sediments derived from the Tombstone batholith, biotite, which may constitute up to 18 percent of the minus-80 mesh fraction of stream sediment, will undoubtedly be an important sorber of $UO_2(OH)^+$.

Streams draining the tinguaite phase of the batholith, however, generally have a pH greater than 7.0 due to an increase in dissolved carbonate. The HCO_3^- in this area is derived from the leaching of calcite that is finely dispersed within the tinguaite. Although the carbonate ion concentration is large enough to increase the pH, it is still too low to complex significant proportions of the total dissolved U. The increased

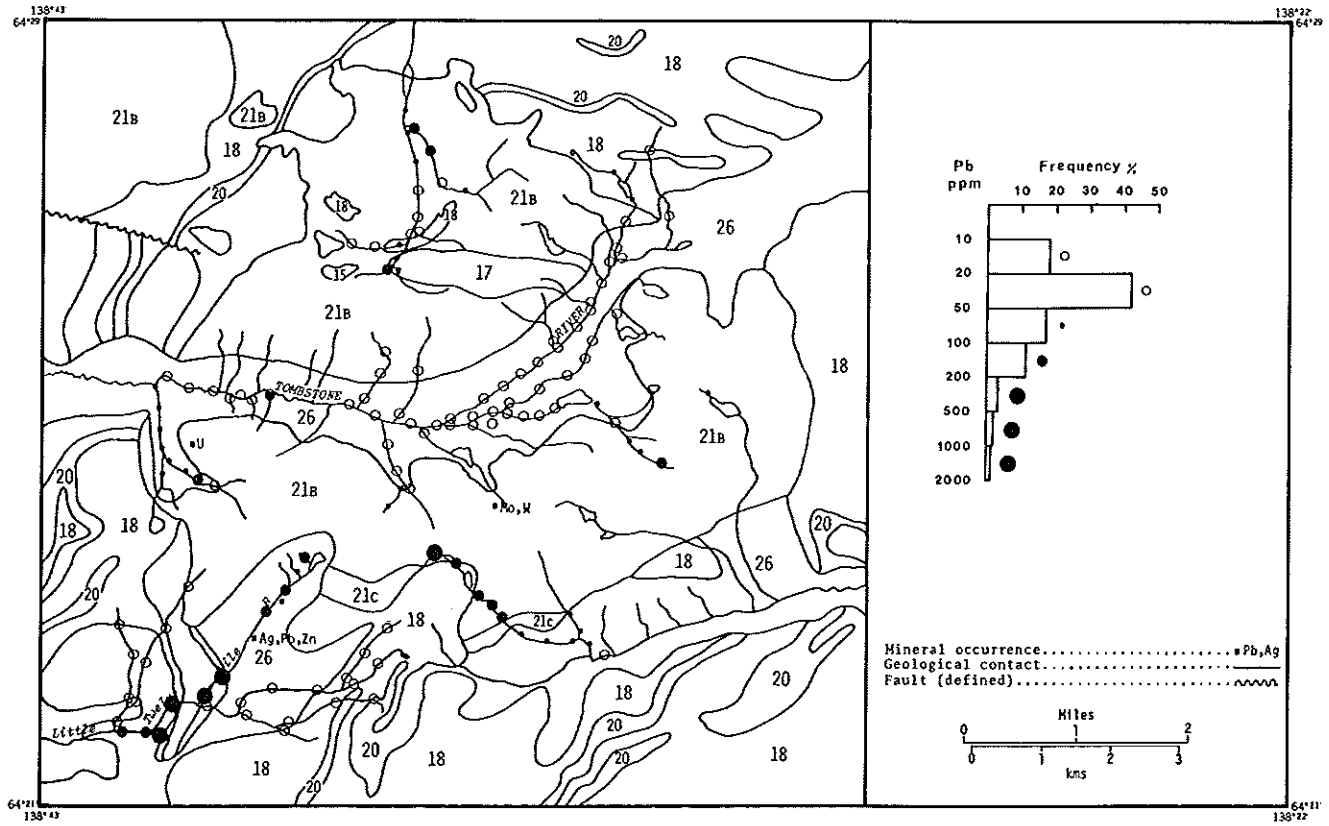

FIGURE 13. Distribution of Pb in sediments (minus-80 mesh) from streams draining the Tombstone batholith.

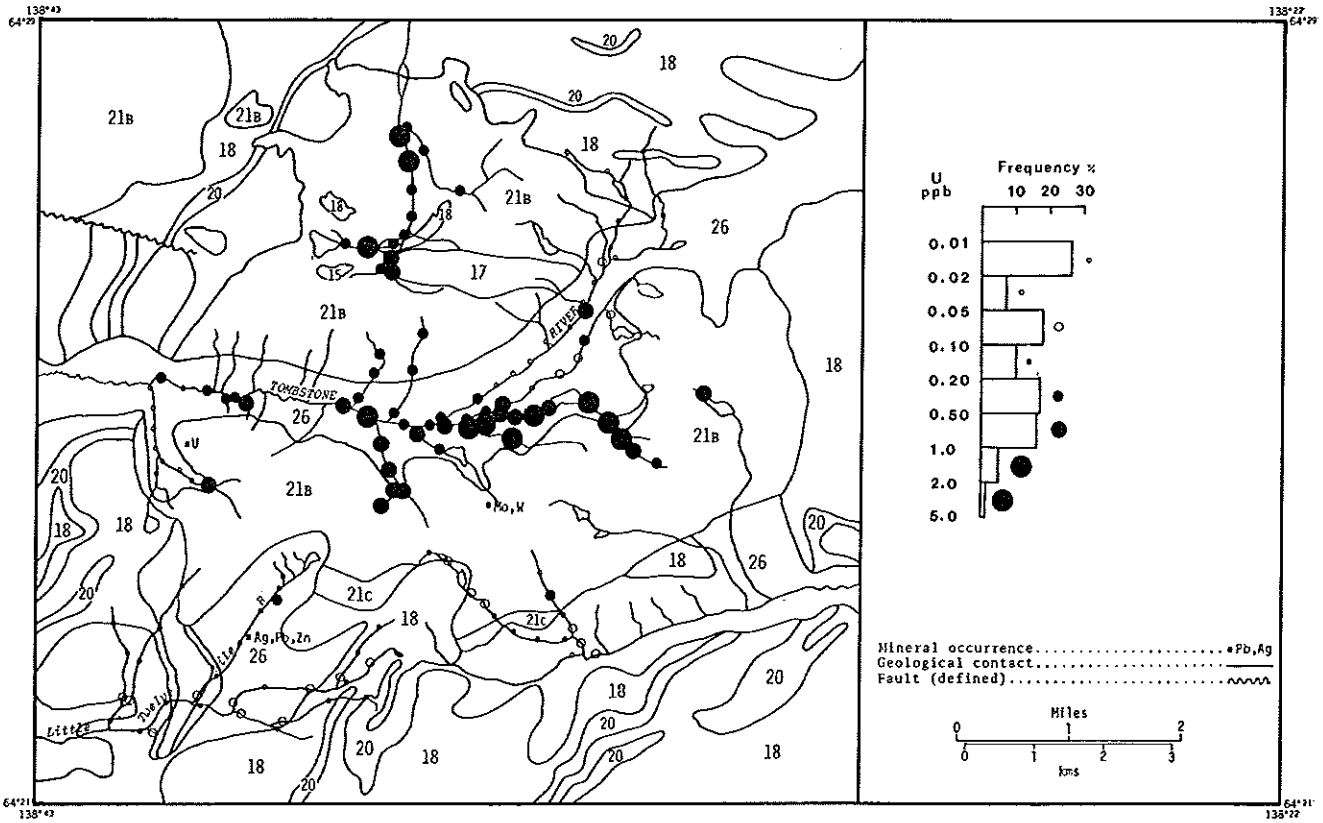

FIGURE 14. Distribution of U in waters from streams draining the Tombstone batholith.

pH, however, serves to further hydrolyse UO_2^{+2} to $UO_2(OH)_2$ which either precipitates or is sorbed from solution (Figure 15). Therefore, U occurring as uraninite in the tinguaite may be expected to be oxidized to uranyl ions and deposited before being transported far in stream waters. Consequently, most of the U in this area will be of mechanical derivation and will be impoverished with respect to sediments that contain an added component of hydromorphically derived U. The negative correlation of pH (and HCO_3^-) with U in both stream sediments and waters (Table 5) may result, therefore, from the destabilization of U in solution by the formation of $UO_2(OH)_2$ with increasing pH (Seregeyeva, *et al.*, 1976).

The presence of pyrite within the tinguaite may also influence the dissolution of uraninite. The oxidation of pyrite by ground and surface waters would tend to retard the oxidation of uraninite to uranyl ions.

The U occurrences associated with the tinguaite phase of the Tombstone batholith contain high concentrations of both Pb and F. The distribution of F (Figure 16) in stream waters delineates areas of fluorite-bearing tinguaite. The source of F in streams intersecting the syenitic core is less clear although the possibility of tinguaite occurring as part of a roof pendant now covered by glacial deposits should not be ruled out.

The spatial distribution of Pb in stream waters has been discussed previously by Goodfellow and Jonasson (1977). The Pb anomalies are coincident with F and originate from the oxidation and dissolution of galena present in veinlets intersecting the tinguaite. The source of Pb in streams draining the core of the batholith is less well understood, although galena associated with later felsic dikes is a plausible explanation. The distribution of anomalous Cu in stream waters (Figure 17) also corresponds to areas of high U in streams intersecting the southern contact and core of the batholith. These Cu anomalies reflect the presence of chalcopyrite known to be associated with certain U occurrences.

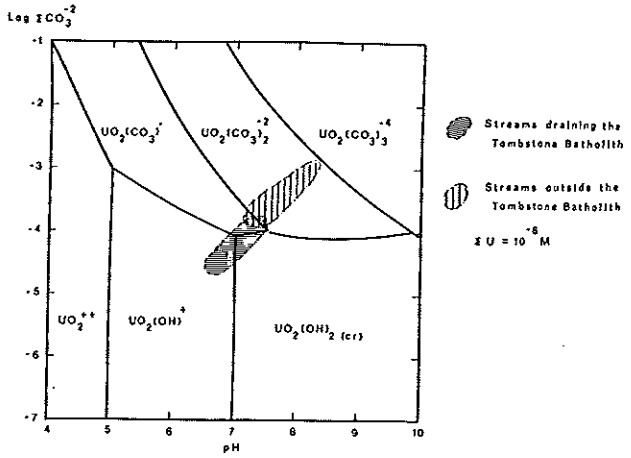

FIGURE 15. Stability fields for uranyl carbonates and hydroxides at 25°C and total U = 10^{-6}M. Waters from streams draining both the Tombstone batholith and surrounding rocks are also plotted.

TABLE 5

CORRELATION MATRIX OF CHEMICAL DATA FOR WATERS FROM STREAMS DRAINING THE TOMBSTONE BATHOLITH

	U	F	pH	Ca	K	Na	HCO_3	Conductivity
Cu	.27	.35	-.27	.01	.13	.12	-.05	.04
Cond.	-.32	-.26	.65	.99	.86	.86	.96	
HCO_3	-.28	-.29	.68	.96	.79	.80		
Na	-.13	.01	.41	.80	.97			
K	-.10	-.06	.37	.80				
Ca	-.32	-.29	.69					
pH	-.46	-.34						
F	.51							

TABLE 5. Correlation matrix of cations and anions in stream waters, Tombstone batholith.

DISCUSSION

The Tombstone batholith represents a composite syenite intrusion in which U mineralization is closely associated with the early phase of intrusive activity. The evolution of the Tombstone magma played an important role in the formation of U mineralization. Unlike other syenitic intrusions, the early crystallization of pseudoleucite generated a peralkaline fluid enriched in alkalies and volatiles. U and other 'agpaitic' metals, such as Pb and Mo in alkaline magmas, usually show a strong affinity for the halogen- and alkali-rich fluid phase (Gerasimovskii, 1968). This is related to the high temperature stability of these metals as fluoride or carbonate complexes as well as their inability to be incorporated into rock forming silicate minerals. The close association of U mineralization with fluorite and hydrous biotite within the tinguaite supports this interpretation. Partial extraction studies on rocks suggest that the U occurs predominantly as easily leachable uraninite.

Although some Th commonly accompanies U during mineralizing processes, Th is however less soluble than and not as mobile as U in alkali-volatile rich magmatic fluids. Moreover, the oxidation of U^{+4} to U^{+6} further promotes the separation of Th and U. This may explain the concentration of U in the more alkaline and volatile-rich tinguaite in close association with fluorite and hydrous biotite, and the relative abundance of Th in the more refractory accessory minerals within the syenite. W and Mo generally

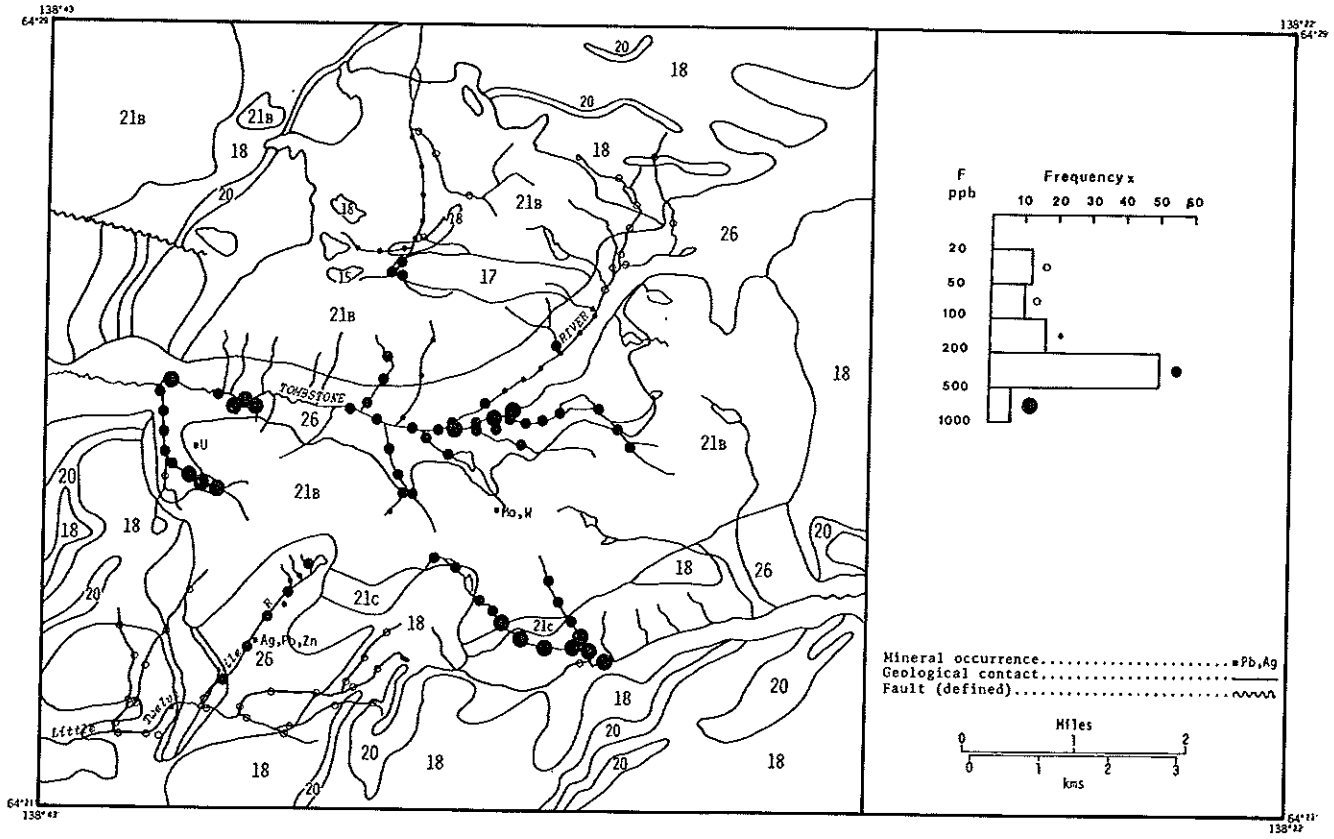

FIGURE 16. Distribution of F in waters from streams draining the Tombstone batholith.

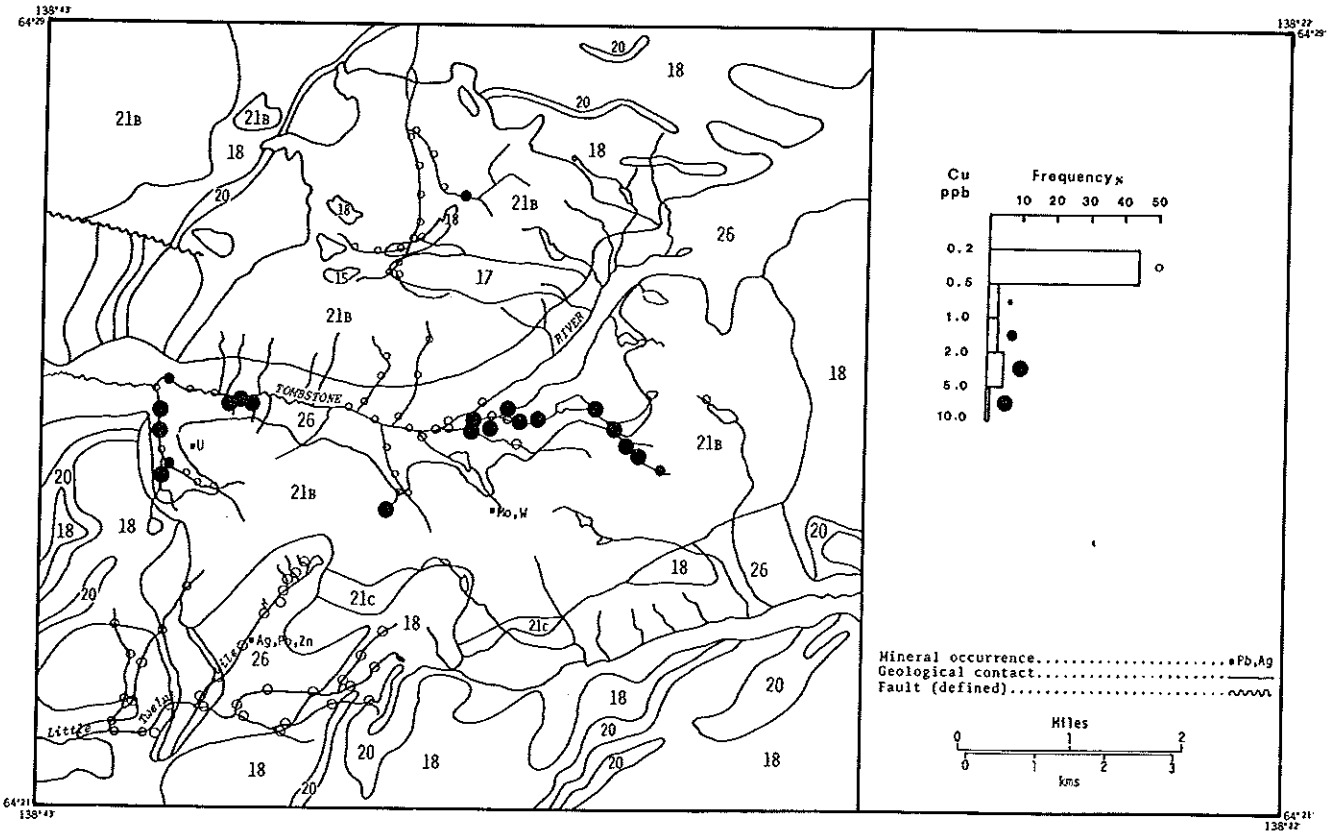

FIGURE 17. Distribution of Cu in waters from streams draining the Tombstone batholith.

show a close affinity with silica-rich residual fluids, which is consistent with the occurrence of molybdenite and scheelite within the quartz monzonite and granite stock and apophyses.

Contemporaneous tectonic activity (faulting and shearing) as deduced from mineralogical features possibly aided the emplacement of the tinguaite and the associated U-bearing halogen-rich phase at relatively higher levels in the crust and generated zones of low pressure which served to localize and concentrate U. The close spatial, temporal and genetic association of U mineralization with the tinguaite along the southern border of the batholith suggests that other occurrences of tinguaite which may be located elsewhere within the batholith constitute prime exploration targets for U and possibly Pb mineralization.

Geochemical anomalies in stream sediment strongly reflect those in bedrock. For example, the U-bearing tinguaite phase of the batholith is outlined by high U, Pb, Mo, and, to a lesser extent, W in stream sediments. In the case of elements such as W that occur as minerals resistant to chemical degradation, their dispersion is due to physical processes. This is supported by the presence of minerals such as zircon, sphene and, in some areas, uraninite in the heavy fractions of sediments. Because of the close association of uraninite with biotite in the tinguaite, the U in the stream sediments occurs most commonly as composite uraninite-biotite grains and is therefore distributed over a large specific gravity range depending on the proportion of biotite present.

The chemistry of stream waters illustrates that the U is also dispersed hydromorphically. The CO_3^{-2} content of the waters in streams intersecting the Tombstone batholith is too low to form significant uranyl carbonate complexes for the measured pH range. Instead, the U is most likely transported as a $UO_2(OH)^+$ complex. With an increase in pH, the U would be expected to be further hydrolyzed and deposited as $UO_2(OH)_2$ on the surfaces of minerals such as micas, clays, and organics due to their large surface charge density. In the case of sediments derived from the Tombstone batholith, the organic matter content is generally less than 10 percent and there is not significant correlation with U.

The results of this integrated lithogeochemical and hydrogeochemical study have considerable implications in exploration for U, Mo, W, Pb and related elements within the Tombstone batholith and other intrusions of similar composition. Elsewhere within the batholith where tinguaite occurrences have been mapped, the strong development of multi-element anomalies of U, F, Mo and Pb are good indicators of mineralization. Other features of exploration significance are extensive shearing, silicification and the development of abundant dark brown biotite and fluorite.

The strong multi-element anomaly at the core of the batholith needs further evaluation. Geochemical data from stream sediments and waters suggest that the anomaly is apparently neither lithologically controlled nor related to environmental factors. Moreover, the anomaly is not related to heavy mineral concentrations nor to the Th-bearing silicates known to occur in the area. The Th content of stream sediments from this anomaly is not significantly different from values obtained elsewhere in the batholith. Moreover, partial extraction studies suggest that the U in the sediments is in a readily leachable form and most likely occurs as both mechanically dispersed uraninite and hydromorphically transported U, a portion of which was subsequently deposited. The characteristic element associations (e.g. F, Mo, Pb) are similar to those obtained in streams draining the uraninite-bearing tinguaite. The presence of a strong W anomaly in the same area may reflect proximity to monzonite dikes which are known to occur in the area and are generally enriched in W. Therefore, the multi-element anomaly located at the core of the batholith may represent a tinguaite source as yet unrecognized and possibly overlain by glacially derived deposits.

ACKNOWLEDGMENTS

We are indebted to Dr. Ian R. Jonasson for his support and useful comments during the execution of this project which forms part of the Uranium Reconnaissance Program (URP) being undertaken by the Geological Survey of Canada. We also acknowledge the contributions of many of our colleagues. Ms. G.E.M. Hall was responsible for much of the analytical services. Mr. G. Lachance made arrangements for X.R.F. analyses, and Mr. D. Ellwood assisted with the data processing. Financial support was provided by funds from the URP, and a G.S.C. Visiting Fellowship which supported the first author. Critical comments by I. R. Jonasson, R. T. Bell, W. D. Sinclair, and especially D. J. Tempelman-Kluit, have helped in the improvement of the manuscript.

REFERENCES

Armstrong, F. C., 1974. Uranium resource of the future—"porphyry uranium" deposits. Proc. Symp. Form. Iran, Ore Dep., Int. Atomic Energy, Vienna, 625–634.

Bhose, H., Rose-Hansen, J., Sorensen, H., Steenfelt, A., Lovborg, L., and Kuzendorf, H., 1974. On the behavior

of uranium during crystallization of magmas—with special emphasis on alkaline magmas. In: Formation of Uranium Deposits, Int. Atomic Energy Agency, Vienna, 49–60.

Bostock, H. S., 1961. Physiography and resources of the northern Yukon; Can. Geogr. J., 63: 112–119.

Boulanger, A., Evans, D. J. R., and Raby, B. F., 1975. Uranium analysis by neutron activation delayed neutron counting. Proc. 7th Ann. Symp. Can. Mineral. Analysts, Thunder Bay, Ont., 10 p.

Brown, R. S. E., 1960. The distribution of permafrost and its relation to air temperature in Canada and the U.S.S.R., Arctic, 13: 163–177.

Cockfield, W. E., 1919. Silver-lead deposits of the Twelvemile area, Yukon; Geol. Surv. Can., Summ. Rept. 1918, pt. B, 15–17.

Currie, K. L., 1976. The alkaline rocks of Canada; Geol. Surv. Can. Bull., 239: 1–21.

Findlay, D. C., 1975. Map showing the geology and mineral deposits of Yukon Territory and part of the southwest District of Mackenzie, Northwest Territories; Geol. Surv. Can., Open File 87.

Garrett, R. G., 1971. Molybdenum, tungsten, and uranium in acid plutonic rocks as a guide to regional exploration, S. E. Yukon; Can. Min. J., 92: 37–40.

Gerasimovskii, V. L., 1968. Geochemistry of agpaitic nepheline syenites. Proc. 23rd Intern. Geol. Cong., Czechoslovakia, 6: 259–265.

Goldschmidt, V. M., 1954. Geochemistry, Oxford, Clarendon Press, 730 p.

Green, L. H., 1972. Geology of Nash Creek and Dawson map areas, Yukon Territory; Geol. Surv. Canada Mem. 364: 157 p.

Goodfellow, W. D., and Jonasson, I. R., 1977. Geochemical distribution of uranium, tungsten and molybdenum in the Tombstone Mountains batholith, Yukon; Geol. Surv. Can. Rept. Activities, pt. B, Paper 77–1B: 37–45.

Hamilton, D. L., and Mackenzie, W. S., 1965. Phase equilibrium studies in the system $NaAlSiO_4$ (nepheline) $KAlSiO_4$ (Kalsilite)-SiO_2-H_2O. Mineral. Mag., 34: 214–231.

Johannsen, A., 1937. A Descriptive Petrography of the igneous Rocks. Univ. Chicago Press IV: 145–151.

Jonasson, I. R., and Goodfellow, W. D., 1976. Uranium reconnaissance program: Orientation studies in uranium exploration in the Yukon; Geol. Surv. Can., Open File 388, 97 p.

Knight, C. W., 1906. A new occurrence of pseudoleucite. Am. J. Sc., 21: 286–293.

Labhard, T. P., and Rybach, L., 1971. Abundance and distribution of uranium and thorium in the syenite of Piz Giuv (Aar-Massif, Switzerland). Chem. Geol., 7: 237–251.

Langmuir, D., and Applin, K., 1977. Refinement of the thermodynamic properties of uranium minerals and dissolved species, with application to the chemistry of ground waters in sandstone-type uranium deposits. U.S. Geol. Surv. Circ. 753: 57–60.

Le Maitre, R. W., 1976. The chemical variability of some common igneous rocks. J. Petrology, 17: 589–598.

Shal, K., Doe, B. R., and Wedepohl, K., 1974. Lead In: Handbook of Geochemistry (ed.) K. Wedepohl, Springer-Verlag, II-4: 82-E-9.

Seregeyeva, E. I., *et al.*, 1976. Experimental investigation of equilibria in the system. UO_2-CO_2-H_2O in 25–200°C temperature interval. Geol. Reg., 18: 900–910.

Shatkov, G. A., Shatkova, L. N., and Guschin, Y. E., 1970. The distribution of uranium, chlorine, molybdenum and niobium in liparites and acid volcanic glasses. Geochem. Intern., 7: 1051–1063.

Smith, A. Y., and Lynch, J. J., 1969. Field and laboratory methods used by the Geological Survey of Canada in geochemical surveys. No. 11, Uranium in soil, stream sediment and water. Geol. Surv. Can. Paper, 69-40: 9 p.

Tempelman-Kluit, D. J., 1969. A re-examination of pseudo-leucite from Spotted Fawn Creek, west central Yukon; Can. J. Earth Sci., 6: 55–62.

—— 1970. Stratigraphy and structure of the 'Keno-Hill Quartzite' in Tombstone River—Upper Klondike River Map area, Yukon Territory; Geol. Surv. Can. Bull., 180: 102 p.

Tuttle, O. F., and Bowen, N. L., 1958. Origin of granite in the light of experimental studies in the system of $NaAlSi_3O_8$-$KAlSi_3O_8$-SiO_2-H_2O. Geol. Soc. Am. Mem. 74 p.

Upton, B. G. J., 1960. The alkaline igneous complex of Kungna Field; Grønlands Geol. Unders, 27; 145 p.

Vernon, P., and Hughes, O. L., 1966. Surficial geology, Dawson, Larsen Creek, and Nash Creek map areas, Yukon Territory; Geol. Surv. Can. Bull., 136 p.